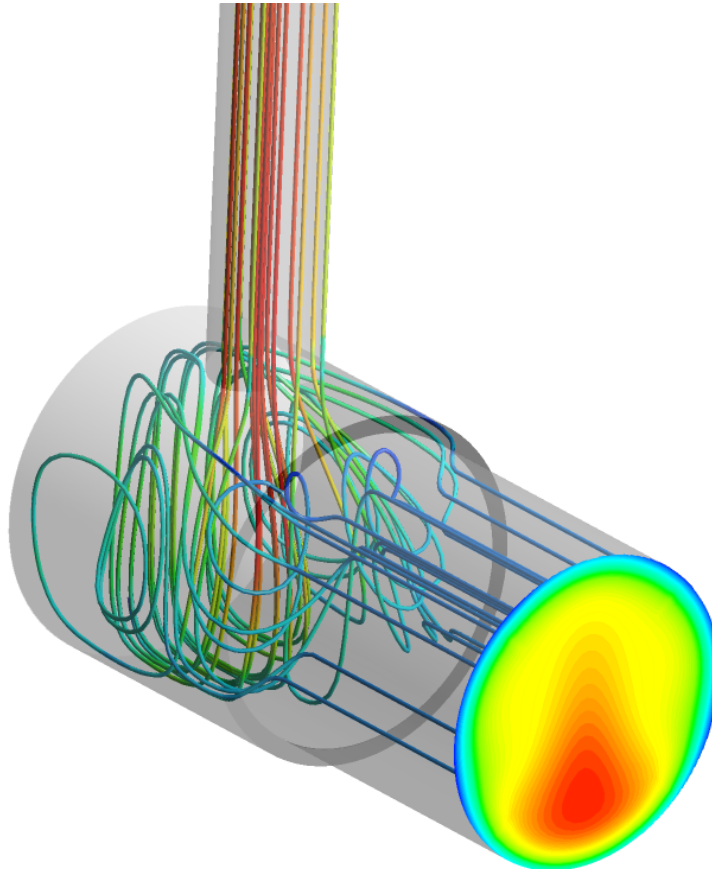




CHALMERS



CFD Simulation of Flow and Temperature inside a monolith of an Exhaust After-Treatment System (EATS)

Master's thesis in Innovative and Sustainable Chemical Engineering

VICTOR DUONG
MOHAMMED AFZAL KHAN

MASTER'S THESIS IN INNOVATIVE AND SUSTAINABLE CHEMICAL ENGINEERING

CFD Simulation of Flow and Temperature inside a monolith of an Exhaust After-Treatment System (EATS)

The report contains a detailed study of CFD modelling of a monolithic reactor in EATS using Ansys Fluent. The simulated flow behavior has been verified and adjusted by laboratory experimentation. Furthermore, a D-optimal design study for finding optimal sensor placements has also been analyzed.

VICTOR DUONG
MOHAMMED AFZAL KHAN



Department of Mechanics and Maritime Sciences
Division of Combustion and Propulsion Systems
CHALMERS UNIVERSITY OF TECHNOLOGY

Gothenburg, Sweden 2019

CFD Simulation of Flow and Temperature inside a monolith of an Exhaust After-Treatment System (EATS)
The report contains a detailed study of CFD modelling of a monolithic reactor in EATS using Ansys Fluent.
The simulated flow behavior has been verified and adjusted by laboratory experimentation. Furthermore, a
D-optimal design study for finding optimal sensor placements has also been analyzed.

VICTOR DUONG

MOHAMMED AFZAL KHAN

© VICTOR DUONG , MOHAMMED AFZAL KHAN, 2019

Master's thesis 2019:57

Department of Mechanics and Maritime Sciences

Division of Combustion and Propulsion Systems

Chalmers University of Technology

SE-412 96 Gothenburg

Sweden

Telephone: +46 (0)31-772 1000

Cover:

The reactor where the streamlines enter from the inlet, with coloring based on velocity magnitude and a temperature distribution is displayed in the outlet of the monolith.

Chalmers Reproservice

Gothenburg, Sweden 2019

CFD Simulation of Flow and Temperature inside a monolith of an Exhaust After-Treatment System (EATS)
The report contains a detailed study of CFD modelling of a monolithic reactor in EATS using Ansys Fluent. The simulated flow behavior has been verified and adjusted by laboratory experimentation. Furthermore, a D-optimal design study for finding optimal sensor placements has also been analyzed.

Master's thesis in Innovative and Sustainable Chemical Engineering

VICTOR DUONG

MOHAMMED AFZAL KHAN

Department of Mechanics and Maritime Sciences

Division of Combustion and Propulsion Systems

Chalmers University of Technology

ABSTRACT

Internal Combustion Engine is the most popular and efficient types of engine used in the transport sector. On the other hand, it has serious downside in degrading the environmental stability as well. The exhaust gases after the combustion of fuel contain emissions which are harmful for human health and responsible for the climate change. Treating the exhaust gases of an Internal Combustion Engine is a major operation in the vehicle. Exhaust After Treatment System engineering simply known as EATS, can treat and remove these substances from the engine exhaust. Although the applied technology in EATS engineering are already very efficient, it is of interest to gather more knowledge about the velocity and temperature distributions inside the monolith of the reactor during transient operation to further improve the efficiency. By using computer aided simulations to capture the fine details, CFD has become a vital part to gain high resolution data in the monolith channels inside an EATS with the single channel approach. However, due to the computational cost, solving for a complete EATS with high resolution is not yet a possibility. The idea behind this research is to find a small set of channels which can be modelled to represent a complete EATS. Hence, using the single channel approach on the selected channels, these can represent a high resolution EATS simulation.

The goal of this project was mainly focusing on obtaining high detailed simulations of flow and temperature for a specially designed monolithic catalytic reactor in transient state. A range of air flow and temperatures were tested in a laboratory, where the flow and temperatures in the inlet and outlet of monolith were recorded. The same flow conditions were reproduced with CFD simulations and a verification for the CFD model was done by comparing these results. A D-optimal algorithm was used on the outlet data of simulated flow tests, to find the optimal four locations for the different cases. Finally, a weighting model was developed where the four locations represent the complete outlet.

Keywords: Internal Combustion Engine, Exhaust After Treatment System, Computational Fluid Dynamics, Design of experiments, D-Optimal analysis etc.

ACKNOWLEDGEMENTS

First of all, we would like to thank each other for this amazing thesis work we've done together in these past 24 weeks. The chemistry between the two of us was absolutely great in the area of cooperation and assisting each other. It was a mesmerizing working experience where both of us have had substantial amount of interest in this topic.

We would like to thank our supervisor Andreas Nygren for his supervision, knowledge sharing and guidance in many turnings of this thesis. Without his assistance, this thesis would not see the light of success and be very hard to reach a desired level.

We want to thank Nikhil Sharma for helping us with the experimental setup and data which we used in our experiments successfully. For his support, our experiment went smooth and quickly.

We are pleased to thank our examiner Associate Professor Jonas Sjöblom for his teaching, instruction, technical discussion, conducting council, direction and motivation behind this research work. From the first day until the submission, his care and ministrations were truly helpful to flourish fully with our talents to reach this level of work in a thesis. We humbly express our gratitude to him.

Finally we would love to thank our family, our parents, siblings and friends for their continuous support and encouragement behind us, which helped us to stay focused and oriented all this time.

Mohammed Afzal Khan and Victor Duong
Gothenburg, June 2019.

ACRONYMS

CFD	Computational Fluid Dynamics
EATS	Exhaust After-Treatment System
ICE	Internal Combustion Engine
GHG	Green House Gas
DOC	Diesel Oxidation Catalyst
DPF	Diesel Particulate Filter
SCR	Selective Catalytic Reactor
DEF	Diesel Exhaust Fluid
ASC	Ammonia Slip Catalyst
SI	Spark Ignition
CI	Compression Ignition
PCA	Principal Component Analysis
PM	Particulate Matter
ISA	International Standard Atmosphere
LPM	Litres per minute
RSME	Root mean square error

CONTENTS

Abstract	i
Acknowledgements	ii
Acronyms	iv
Contents	v
1 Introduction	1
2 Framework	4
2.1 Structure of the thesis	4
2.2 Aim	4
2.3 Applicability	4
2.4 Limitations	5
2.5 Specification of issues under investigation	5
3 Background	6
3.1 Internal combustion engine (ICE)	6
3.2 Exhaust-gas after treatment system (EATS) for diesel engine	7
3.3 Electrification vs Combustion	8
3.4 Driving cycle	8
3.5 Material properties	9
3.5.1 Cordierite	9
3.5.2 Insulation material	9
4 Theory: CFD Modelling and Simulation	10
4.1 Software and tools	10
4.1.1 CAD model	10
4.1.2 FLUENT	10
4.2 Mesh quality	10
4.3 Governing Transport Equations	12
4.3.1 The equation of Continuity	12
4.3.2 The equation of Motion	12
4.3.3 The equation for energy transport	12
4.4 Numerical solvers	13
4.4.1 Upwind schemes	13
4.5 Turbulence modeling	13
4.5.1 Transport equation for Turbulent Kinetic Energy, k	14
4.5.2 Dissipation of Turbulent Kinetic Energy, ϵ	14
4.6 Modelling the Near-Wall Region	14
4.7 Turbulence quantities	15
4.7.1 Turbulence intensity	16
4.7.2 Turbulence length scale	16
4.8 Modelling of the monolith	16
4.9 Space velocity	17
4.9.1 Space velocity into Velocity	17
4.9.2 Space velocity into Mass flow	17
4.10 Simulation	18
4.10.1 Convergence	18
4.10.2 Residuals	18
4.10.3 Under-relaxation factor (URF)	18
4.10.4 Grid independence	18

5 Theory: D-Optimal Design	19
5.1 Principal component analysis(PCA)	19
5.2 Unit-variance scaling	19
5.3 D-optimal design in MATLAB	19
6 Setting up a simulation	20
6.1 Initial conditions	20
6.2 Turbulence quantities	20
6.3 Boundary Conditions	20
6.4 Incompressible ideal gas density	20
7 Experimental Methodology	22
7.1 Preliminary experimental limits	22
7.2 Experimental Setup	22
7.2.1 Experimental arrangement	22
7.2.2 Experimental flow chart	23
7.2.3 Images of Equipment	23
7.2.4 Functions of the equipment	24
7.2.5 Laboratory view	25
7.2.6 Position of Thermocouples	26
7.3 Experimental procedure	27
7.3.1 Experiment 1: Observation of velocity profiles	27
7.3.2 Experiment 2: Testing of proposed flow conditions	27
7.3.3 Experiment 3a: Reactor cooling in three flow conditions	28
7.3.4 Experiment 3b: Reactor cooling in two flow conditions	28
8 Adjusting The Model	29
9 Processing Temperature and Velocity sensor data	30
10 Optimal Sensor Locations	31
11 Results and Discussions	32
11.1 Initial Simulation Model	32
11.1.1 Pressure drop	34
11.1.2 Grid independence	34
11.2 Experiments	35
11.2.1 Experiment 1: Observation of velocity profiles	35
11.2.2 Experiment 2: Testing of proposed flow conditions	35
11.2.3 Experiment 3a: Reactor Cooling in three flow conditions	37
11.2.4 Experiment 3b: Reactor Cooling in two flow conditions	37
11.3 Adjustments to the model	38
11.3.1 Comparison of steady state temperatures between experiment and simulation	39
11.3.2 Transient cooling	42
11.4 Optimal sensor locations	42
11.4.1 Potential sensor placements	42
11.4.2 Principal component analysis	43
11.4.3 D-optimal design	44
12 Conclusion	47
13 Recommendations	48
14 Future work	49
References	50

A Appendix A	52
A.1 Expected highest temperature in the monolith outlet	52
A.2 Experimental Risk analysis	53
B Appendix B	55
B.1 Mesh	55
B.2 Grid independence study: Velocity distribution	56
B.3 Grid independence study: Temperature distribution	57
C Appendix C	58
C.1 Additional Figures	58

1 Introduction

Transportation has been one of the biggest contributors (Currently accounts for around 28%) of total Green House Gas (GHG) emissions in the world [1]. Internal Combustion engine (ICE) is the most popular form of engines used in the transport sector and it is the main reason for emitting human health and environmental degrading substances. Studies have found that the exhaust gases of ICE can cause lung damage, respiratory complication and even cancer. After the burning of fuel for power production in ICE, the exhaust gases such as carbon dioxide (CO₂), particulates are the dominant factor for contributing to climate change. CO₂ is causing severe environmental threat such as global warming. Rising of sea level, smog formation, acid rain, reducing visibility, extreme heat waves, long drought, unusual weather behavior etc. are some of the effects from climate change [2]. Rapid increase of using motor vehicles as well as without, inadequate use or unavailability of proper emission control technologies are leading to this dangerous situation in the upcoming decades. Outdoor air pollution holds for around 4.2 million human death world wide every year and contributes to 7.6% of all deaths in 2016 estimated by WHO in their 2018 annual report. [3] As it is seen that emission from transport sector is causing an enormous amount of damage to the human health and environment, improving emission control technology is a must to save the planet.

As mentioned before, ICE is the most common type of engines used in modern transport vehicles. Although in recent years, the electrification of light duty vehicles has escalated substantially, there is still arguably no better alternative to the combustion engines for heavy duty vehicles. Combustion engines are very much efficient in converting workable energy from the fuel. They are also good for long haul drive, reliability and availability of fuel. But they have some important downside as well, such as emission from the exhaust after the combustion of fuel. Spark-Ignition and Compression-Ignition are two types of ICE which use petrol and diesel as fuel respectively. Although diesel engines emit less amount of CO₂ than petrol engines, they emit other dangerous substances like nitrogen and particulates. As per emission legislation, the exhaust gases has to be treated before releasing into the environment.

Emissions from automotive engine's exhaust are mainly carbon mono and di-oxide, hydrocarbons, particulates and nitrogen oxides. EATS is a solution for automotive engine to treat these gases and is also a requisite to meet the emission legislation. The principal function of EATS for an ICE is to treat and remove the exhaust gases from the engine by catalytic reduction after the fuel has burned. There are three primary components in the engine to treat the exhaust gases: Diesel Oxidation Catalyst captures the carbon mono-oxide and hydrocarbons, Diesel Particulate Filter System removes the particulates and finally a Selective Catalytic Reduction System removes nitrogen oxides. To reach a higher conversion and achieve zero net emissions, an improved modelling of flow patterns and temperature distributions inside the EATS is needed.

This Master's thesis focused on the study of exhaust gas flow and temperature profiles in a monolithic reactor inside Exhaust After Treatment System, known as EATS. The study helped to put sensors in optimal locations in the monolith, which determined the state of the reactor, by having a better understanding of these distributions. Although EATS for combustion engines are already very efficient in treating exhaust gases, still more research study and improvement is needed to achieve a complete efficient and easily available technology which can be implemented to not only in developed countries but also in developing countries. For light duty automotive application, electrification is trying to solve the emission problem substantially yet not enough because of the inefficiency, lack of technological advancement and high costings. But for heavy duty application, electrification technology has to go a long way to take over combustion technology. Pursuing to stay below the 1.5°C limit of the global temperature, a significant reduction of emission from the exhaust of combustion based automobile engines is needed.[1]

To understand the effect of exhaust gases conversion inside the catalyst, modelling the flow is needed. Computer aided simulation modelling is a popular way nowadays to reduce the cost of unnecessary experiments. Single channel approach is the most general way to do the modelling of catalyst. But this approach does not take into consideration the temperature variation inside the catalyst. It only shows the flow's characteristics in one single channel of a monolith. In reality, heat conduction between the channels of the catalyst also occur. That is why, multi-channel modelling approach is a more realistic way to model the flow in a catalytic converter. In fact, it is a realistic supplement of the single channel approach. It is done by simulating the

flow in the catalyst with a single channel approach while heat flux between the channels are taken into account.[4]

But there are some modelling complication to do the multi-channel approach. It is very difficult to simulate a complete monolith with thousands of channels because of heavy computational effort i.e. massive cost and huge computational time. Our investigation will focus on finding the optimal sensor locations out of the thousands of channels of monolith, which will represent the flow's characteristics in the whole monolith. In this thesis, multi-channel approach (a few number of channels) with radial heat conduction between the channels, had been taken into account to understand the flow characteristics inside the monolithic reactor.[4]

The goal of this project was mainly focusing on simulating the flow and temperature distributions inside a specially designed reactor, which contains a ceramic monolithic catalyst substrates made from cordierite. Cordierite is a magnesium-alumino-silicate ceramic material widely used to produce emission control catalysts. [5] The exhaust gas enters into the reactor with a bend and flows through the monolith. It is of interest to gather more knowledge about the distributions of velocities and temperatures during the transient operation of various flow conditions and temperatures. Another important goal of the project was to place sensors which can capture the flow and temperature distributions in the monolith. After gathering the information of those above mentioned profiles, sensors was installed in optimal locations for the purpose of extracting the most amount of information. To fulfill the goal of this masters thesis project, the following situations were investigated.

The project started with modelling the reactor by defining the system's dimensions in ANSYS Workbench, which is a vastly used software for CFD simulations. Meshing the geometry is one of the most crucial part in the field of CFD. It is the process of dividing the whole domain into small cells or parts for distributing the information uniformly throughout the domain for the purpose of computational accuracy. Checking grid independence is a good practice in CFD study, which means different meshing will not affect the computational accuracy and will produce similar results. Grid independence study for different mesh sizing (a hundred thousands cells to one million cells for the whole domain) was done in this thesis to run the simulation in larger cell size for reducing computational time and effort, as coarser the mesh, heavier the computation. The various zones such as inlet, outlet, walls, interiors and interfaces of the domain has to be defined as well. After the meshing, simulation was set up in ANSYS Fluent software. Setup the simulation had to be carried out carefully by thoroughly thinking and understanding the physics of the domain. As Ronnie Andersson mentioned in his book "Computational Fluid Dynamics for Engineers",

"Without proper understanding of the CFD program and the modelling theory behind it, CFD can become limited to colorful fluid display."[6]

For setting up the simulation, turbulence model was chosen first. In our case, the popular k-epsilon model was chosen as it can handle high Reynolds number flows. As there was no swirling flows, but there was a round jets in our case, the modified Realizable k-epsilon model was selected instead of the modified RNG or standard k-epsilon model. Modelling the near wall region is also crucial as solid wall possesses significant affect in turbulent flows. There are two ways to model the near wall region. It can be modelled either with wall function approach, where it will work as a bridge between the wall and fully turbulent region; or with the near wall model approach, where the turbulence model will be modified to resolve the viscosity affected region all the way to the wall with finer mesh. The materials for the different parts of the body was chosen with correct physical parameters. The physical parameters of the catalyst was chosen from reliable sources as the flow would be affected greatly by the physical characteristics of monolith. By defining boundary conditions of the simulation with the relevant ranges for flow, temperature, pressure gradient, heat conduction on the wall and convection inside the monolith, the simulation was ready to start. To observe the simulation, various monitoring activity for a wide range of parameters prior to the calculation had be defined.

At first a steady state simulation was carried out to analyze the different measures of the system such as flow uniformity, max gradient, variances to investigate distributions across the reactor. After achieving preliminary knowledge from the steady state simulations, transient simulations had been carried out considering temperature and flow as variables to investigate distributions of velocity and temperature across the reactor.

Subsequently to the computer simulated experiments, laboratory experiments were executed to observe the velocity and temperature profiles in the reactor and compare these results with the simulation. Three different

experiments were done in Chalmers combustion department's laboratory. In the first experiment, different flow conditions were tested to capture the velocity profiles in the monolith. The second experiment was done to run the proposed flow conditions of the exhaust gases described in detail later in the report. The last one was reactor cooling experiment where the cooling effect in the reactor for different flow conditions had been carried out. Therefore, the experiments were done with a range of flow conditions and temperature of air to capture the velocity and temperature profiles in the monolith. Using the results from the experiment, the CFD model was adjusted to mimic the real values. After adjusting the model with experimental data, a D-optimal design study had been conducted for finding the optimal sensor locations to express the state of the reactor. D-optimal study provides the locations of the sensors which extract the most amount of information from the mentioned profiles.

Since this Master's thesis was only focusing on the velocity and temperature profiles of the flow entering into the reactor, the exhaust gas was assumed to be pure air which is not true in real life. Reactions of the exhaust gas components is a decisive part of the study of CFD simulation of EATS system, which was not added as well in this project. These decisions were made for the sake of simplicity and lack of time. As a result, reactions will be offered as a future continuing work to this project.

2 Framework

In this chapter, the layout of the project will be discussed. It will clearly describe the applicability, goals and limitations of the project. This chapter will also reflect the types of questions this project will answer.

2.1 Structure of the thesis

The process view of this thesis will be presented here as following.

- Setting up a CFD model of the system.
- Setting up the experimental rig in the laboratory with temperature sensors (thermocouples).
- Conducted different laboratory experiments with a range of velocity and temperature to observe these distributions in the reactor.
- Using data from the Cooling experiments to fit the heat transfer parameters in the CFD model.
- Simulate the proposed driving cycle and extract velocity and temperature data from 82 possible sensor positions designed in the CFD model.
- Performed D-optimal design study with PCA to extract the best representative channels (sensor locations) to be used in a weighting model.

2.2 Aim

The objective of the project was to develop a better understanding on the behavior of the exhaust gas flow during transient operation while entering into a catalytic reactor with a bent. The variables of interest were temperature and velocity distributions throughout the reactor. CFD modelling and simulation were carried out by ANSYS Fluent software to achieve this goal. Laboratory experiment was conducted alongside for various flow conditions and temperatures in the catalytic reactor to observe these profiles. The simulation model was then adapted with the experimental findings. Finally, a crucial task in this project was also, with simulated data, to find the optimal locations by D-optimal design studies. The sensors are needed to monitor and represent the state of the reactor outlet by applying the relevant knowledge of the flow and temperature distributions in the monolithic reactor.

2.3 Applicability

The sample specimen of the reactor provided, is situated in the DOC unit of an EATS. The exhaust gases from the engine enter into the DOC with a bend. The temporal and spatial distribution of flow velocity and temperature of the exhaust gas will be investigated when it enters inside the reactor. However, the main target of this study is to inspect these above mentioned profiles inside the reactor, regardless in which EATS units it is being positioned. Therefore, this study is applicable to any reactor nonetheless its position in whichever EATS units.

Moreover, it had been assumed that exhaust gas was pure air. As a consequence, reactions of the exhaust gases were not taken into account in this research, only the characteristics of above mentioned profiles in the reactor. Reaction is a very important criterion in EATS study as exhaust gases contain various substances such as CO_x , particulates and NO_x , which react accordingly to different kind of monolith used to capture them sequentially. But learning the flow and temperature distributions in the reactor is the first step to understand the state of the system. As discussed earlier that pure air was considered as exhaust gas ignoring reactions, this project can be applicable to any exhaust gas flow having varying substances in any EATS units.

2.4 Limitations

Reactions are supposed to occur when exhaust gas passes the monolith channels. In the real catalytic reactor, the thermal gradient would potentially give rise to reaction rate differences throughout the reactor due to temperature. The amount reacted would also differ due to residence time difference in the monolith channels. Since the goal of the project is to find the behaviour of the flow and temperatures and thus the optimal placements for sensors, and for the sake of simplifying a very complex system, catalytic reactions will not be accommodated for in this project. It will be offered as future work to this project.

The heater used in the experiment has a capacity of only 3kW. Thus heating the air to an extremely high temperature and study the temperature profiles for it could not be done even with the heater's highest capacity. For a comparative high and medium gas flow, the highest temperature achieved was 220°C and 300°C respectively. The simulation temperature was also adjusted according to the experimental parameters and will also be limited to the same temperatures. The reactor has a fixed volume of 0.6 litres, which also differs depending on type of vehicle.

2.5 Specification of issues under investigation

- What physical phenomena are relevant and need to be implemented and resolved in the CFD model?
- What are the assumptions needed to initiate the simulation and why?
- How are the temperature and flow distribution described in the catalyst?
- How can the transient and steady state be modelled?
- How can the simulation data be trusted?
- How will the locations of sensors in the simulation be done?
- How will the experimental calibration of data be done? How reliable are those data? How will they be acquired?
- How accurate are the experimental results?
- How will the experimental data be implemented in simulation?
- How the adjusted simulation data will be used to find the D-optimal studies of sensor locations?
- How are the final best sensor locations chosen from the sensors in the simulation model?
- Where is the best placements for the sensors? How many sensors are needed? How well can they describe the state of the system?

3 Background

In this chapter, the background information needed for this thesis will be discussed thoroughly.

3.1 Internal combustion engine (ICE)

Combustion or burning of fuel occur inside the combustion chamber of an ICE. The principle of an ICE is to convert chemical energy into useful mechanical work. It is the most common form of engine used in vehicle, in both light and heavy duty applications. There are two types of ICE when ignition of fuel is taking into consideration: spark ignition (SI) engine, which generally follows the Otto cycle using spark plugs to ignite the gasoline (petrol) fuel; and compression ignition (CI) engine, which follows diesel cycle using highly compressed hot air to ignite the diesel fuel.[7]

The CI engine consists of a combustion chamber where the combustion of fuel takes place; an inlet valve which allows the air to go inside the combustion chamber; a piston which moves upward and downward direction inside the chamber for the compression and expansion mechanism and transmit the force to the crankshaft generated in the combustion process; a crankshaft which converts the reciprocating motion of piston into rotary motion; a connecting rod connects piston and crankshaft; an injector which breaks the diesel fuel into very small particles and push them into the combustion chamber; and an exhaust valve which allows the exhaust or burnt fuel to go out of the chamber. There are four principle mechanism of a four stroke CI engine. In the first stroke, called the Intake or Suction stroke, the suction of air takes place through the opened intake valve. The piston moves downward in this stroke which expands the chamber and let the air comes in. The second stroke is called the Compression stroke where the intake and exhaust valve both are closed and piston moves upward compressing the air inside the chamber. This high pressurized compression of air result in increase of air temperature to a level where the burning of fuel can occur. This stroke is followed by Power stroke, where the atomized diesel particle is pushed into the chamber from the injector and fuel starts to burn by the hot compressed air. The combustion of fuel produces exhaust gas which creates a force inside the chamber leading to the downward movement of piston and the expansion of chamber takes place. Power is only produced in this stroke. Finally, in the Exhaust stroke, the piston moves upward and pushes out the burnt gas through the exhaust valve opening.[7]

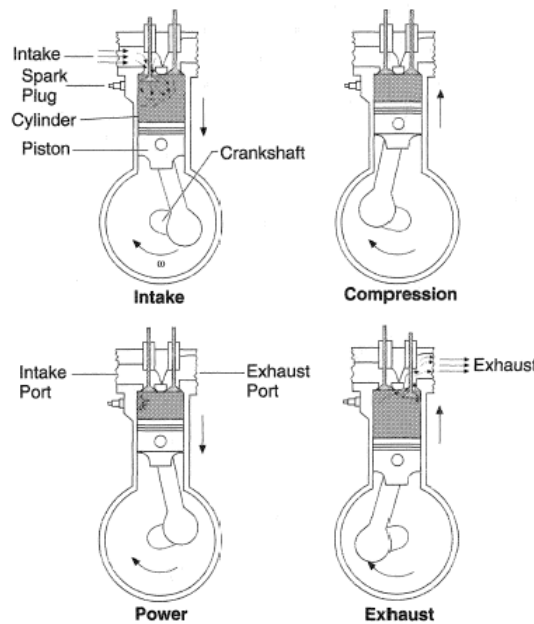


Figure 3.1: A four stroke CI engine with its principle steps. Arcoumanis Dicos. From [8]

When diesel engines were first introduced into vehicles, diesel was considered the future fuel to replace gasoline

(petrol) due to its many impressive features.[9] For instance, diesel has better lubrication property, distilled directly from petroleum and generates less waste heat in exhaust. Additionally, diesel has higher energy density and a lower amount requirement to do the same work as petrol. Cetane ratings is an indicator of the quality of diesel. It indicates the easiness of self ignition. It is inversely proportional to the fuel's ignition time delay, the time between the injection of fuel into the combustion chamber and the beginning of combustion process. Higher the cetane number, quicker the fuel burns. In other words, higher cetane number means the fuel requires less time for the combustion process to be completed. Fast burning of fuel is an important characteristics of fuel and diesel has this very crucial advantage over gasoline.[10]

Besides, CI engines have a higher compression ratio, which is a parameter describing the ratio between the maximum and minimum volume inside the combustion chamber in an engine. It is desirable to have a high compression ratio since higher ratio results in better thermal efficiency, which extracts more mechanical energy from the air-fuel mixture; as higher compression ratio helps to reach the same level of combustion temperature with a less amount of fuel [7][10]. Moreover, CI Diesel engine has a higher thermodynamic efficiency (45%) of converting chemical energy into mechanical energy whereas, which is around 30% in gasoline engine.[7]

One of the most impressive features of a CI diesel engine is that it emits less amount of carbon-dioxide. Even though, combustion of diesel yields less carbon-dioxide, it was found to emit a significant amount of nitrogen oxides (NO_x), carbon mono-oxide (CO) and additionally other particles counted in particle numbers [7][10]. In last 15 years, the emissions of diesel engines have reduced with approximately 95% with main focus on optimizing the combustion. Nevertheless, to meet the emission requirements of tomorrow, further improvements in reducing CO, particulate and NO_x emissions are necessary. Therefore, research and development for improving the exhaust-gas after treatment system has elevated significantly.[11]

3.2 Exhaust-gas after treatment system (EATS) for diesel engine

The EATS unit is situated after the engine compartment. Right after the combustion of fuel, the exhaust gases come out of the engine and enter into the EATS for purification. Here is a picture of EATS unit in a powertrain shown below.



Figure 3.2: Volvo Truck's one box EATS design. Kim Nguyen. From [12]. The left one shows the whole powertrain and the right one shows the EATS unit

The exhaust gases coming from a diesel engine typically contains HC, CO, NO, O_2 and soot. Soot is a collection of carbon particles commonly known as particulate Matter (PM), produced from the incomplete combustion of HC. These exhaust gases need to be treated before releasing into the environment as these have adverse affect on human health and on environment. EATS is a system consists of multiple operation units to reduce these hazardous substances. The fuel type is a major factor on what operations in EATS will consist of. Generally in a modern heavy duty diesel engine, there are five units working sequentially to treat the exhaust gases after the combustion describes as follows:

- Diesel Oxidation Catalyst (DOC): At first, the exhaust gases enter into the DOC unit. This unit oxidizes HC and CO into CO₂ and H₂O. It also oxidizes NO into NO₂ which will be used for the regeneration of DPF and SCR reaction. The regeneration process empties the filter from the soot, otherwise a soot cake is formed in the filter. The increasing amount of soot can create a high pressure in DPF which will eventually increase the fuel consumption slightly, which is why soot needs to be removed by regeneration process.
- Diesel Particulate Filter (DPF): In this unit, soot known as PM from exhaust gases, is collected and oxidized into CO₂ using NO₂ as an oxidizer which was produced in DOC. DPF removes most of the particles from the exhaust, around 99%.
- Diesel Exhaust Fluid/AdBlue (DEF): NH₃ is added into the remaining exhaust gases by this unit. It has to be introduced into the system evenly to achieve a maximum removal of NO_x from the exhaust gases.
- Selective Catalytic Reduction (SCR): After NH₃ is added to the exhaust gas stream, the exhaust gases contains NO_x and NH₃. This unit reduces NO_x into harmless N₂ and H₂O by using NH₃. It removes around 98% of NO_x from the exhaust stream.
- Ammonia Slip Catalyst (ASC): To remove the NO_x from the exhaust stream in the highest possible amount, NH₃ is often injected too much in the DEF step, which cannot be released in the environment and needs to be treated. This unit as a final step of exhaust treatment, oxidizes NH₃ into H₂O and N₂.

The ideal remaining substances after the EATS are CO₂, N₂, O₂ and H₂O which is released to the environment. [13]

3.3 Electrification vs Combustion

Internal combustion engines are not necessarily fuelled by petrol or diesel, renewable energy sources such as alcohol based fuel in SI engine and vegetable oil in CI engine can also serve the same purpose [7]. But to meet the huge demand by supplying the renewable fuels according to it, is the toughest job to do for now. The unavailability of renewable energy source, supplying the processed fuels and costings are the biggest challenge in this matter.

Again, it is very challenging to achieve a zero emission with a high efficiency in diesel engine. In recent years, combustion engine is combined with electrification in passenger cars, but for heavy duty applications, as mentioned earlier, there is no alternative to diesel engine till these days. The drawbacks of electrification are inefficiency, lack of energy storage capacity, short driving range, longer refueling or recharging time, lack of infrastructure such as recharge points, unsuitable for regions facing power shortage etc. [14] It will take a significant amount of research, time, financial support and transport system overhaul to a complete transformation of electrification in transportation sector. Specially in heavy duty application, it seems to be a very hard job to do so.

As combustion technology has lots of advantage over electrification, EATS engineering is the best possible way to combat against the adverse affect of combustion emission. EATS technology has already been implemented and in operation, it just need to be more efficient and available for implementation everywhere in the world. Therefore, the development of EATS engineering is considerably highly preferred before moving into a complete electrification in heavy duty engines.

3.4 Driving cycle

Driving cycle is represented as a set of data points containing vehicle's speed vs time. It is considered as a standardized method to test vehicle's performance such as fuel economy and emissions. Vehicle manufacturers use this method to meet the requirements of emission standard and test procedure. Method of driving cycle changes over time, countries, organizations, with various type of road infrastructure, speed limit policy, technological difference and so on. Nowadays, it has been used widely in vehicle simulation to observe and predict the overall performance of IC engine.

A driving cycle is therefore a set of repeatable vehicle operations for a fixed amount of time and distance. These operations include acceleration, deceleration, constant speed driving, braking, gear shifting through a time and distance. These operations varies by vehicle type, fuel type, mileage, vehicle weight, road condition, gradients of roads etc. Emissions from the vehicles are dependent and thus detected on these above mentioned parameters.[15]

There are two types of driving cycle considering vehicle's speed and weight, Transient Cycle and Modal or Steady State Cycle. Transient driving cycle is based on variable speed of vehicle of on-road driving conditions whereas, modal driving cycle is based on constant velocity segments with constant acceleration and deceleration which is not a representation of real driving condition.[16] Steady state cycle is generally used for heavy duty vehicle whereas transient cycle is used for light duty vehicles. There are many standardized method of driving cycle that are implemented. A detail of around 200 driving cycles will be found on the TRL published project report "*A reference book of driving cycles for use in the measurement of road vehicle emissions*"[15].

Various emission factors must be considered in all types of emission model. Average speed of the vehicle through a fixed time is one of the most familiar technique to asses engine emissions. Emission factor is usually expressed as grams per vehicle per kilometer (gm/vehicle·km). It is measured according to the average speed in a few number of vehicles through different driving cycle. But nowadays, not only average speed of various driving cycles, but also real life traffic and road condition are taken into account when measuring emission factors as they give proper emission measurements.[15]

As mentioned earlier, driving cycle considers vehicle's speed with respect to time, and our project is mainly based on finding the velocity and temperature gradients in the reactor by experimenting various flow conditions of exhaust gases when entering into the reactor with a bend, a standardized driving cycle which shows clearly the relation between exhaust gas velocity according to the vehicle's speed was difficult to find. Furthermore, whereas vehicle's speed is expressed as (km/h), exhaust gases velocity is expressed as space velocity (h^{-1}), definition can be found in 4.9. As a result, we created our own driving cycle or flow conditions in litre per minute (lpm) of exhaust gases considering the space velocity of exhaust gases according to it.

Typically the exhaust gas flow rate for heavy duty truck has a range of 15 to 125 (m^3/h) i.e. 250 to 2000 (lpm). Diesel engine exhaust flow has a space velocity range of 60 000 to 150 000 (h^{-1}).[17]. For the provided 0.6L catalytic reactor, flow conditions according to the space velocity was found by experimenting in the laboratory for our project. The detail description of proposed driving cycle i.e. flow conditions of exhaust gases can be found in 7.3.2 with a pictorial representation in 7.6.

3.5 Material properties

The materials involved in this projects are such as a steel-tube reactor with a cordierite honeycomb monolith which is insulated and fastened by a insulation glass wool material. Properties of steel is easily found on internet while the other two less common materials have to be searched for. The needed properties of the materials are thermal conductivity, density and specific heat capacity.

3.5.1 Cordierite

The thermal conductivity in honeycomb cordierite monoliths are divided into axial and radial direction. Data for general cordierite honeycombs were found, where the radial thermal conductivity is half of the conductivity of axial direction[5]. This is accounted for in FLUENT by using the option orthotropic conductivity, where thermal conductivity is divided into three orthogonal directions. The density and specific heat was found to be 279 [kg/m^3] and 1050 [$J/kg \cdot K$] respectively.[5]

3.5.2 Insulation material

The glass wool insulation material surrounds the monolith. The first purpose of it, is to hold the monolith in place, secondly it reduces the heat losses due to the low thermal conductivity in the glass wool. The exact data were not found on the actual thermal conductivity and specific heat and are instead approximated with air properties except for density which was found to be 380 [kg/m^3].

4 Theory: CFD Modelling and Simulation

This chapter consists of a short description of important concepts and tools which are be a relevant in generating a model with a good and accurate results.

4.1 Software and tools

The simulation part of this project is done with Ansys Workbench. Ansys workbench consist of programs for designing with CAD, dividing the geometry into computational cells(meshing) and to run CFD simulations.

4.1.1 CAD model

The measurements in the drawing of the geometry is directly measured from the real muffler, however there are minor simplified differences which are believed to cause more harm than good in terms of meshing and calculation, when causing inconsistent computational cells in the geometry. A long steel pipe will also be added in the inlet to replicate an extended inlet. The pipe will be chosen to be sufficiently long, in order to achieve a fully developed velocity profile before entering the muffler. To accommodate for the outflow setting used in FLUENT, the outlet is also extended so that the outflow is fully developed before exiting the simulated domain.

4.1.2 FLUENT

Fluent is a software where the calculations will be done and will be the main software that run simulated experiments. Before the real reactor is attached with a pipe, a goal is to make a running model with initial conditions close to the real system for a smoother transition later on when real experimental data is gathered. The process of building the solving model involves both deciding how certain mathematical equations are solved, and also how they are solved. In this project, the equations will be solved with RANS, thus in a continuum which is the most common framework in single-phase fluid mechanics. In fluent, the mathematical models and solvers are chosen as different options, hence it is important to know what models are used and if they are suitable for a specific case.

4.2 Mesh quality

A mesh is a computational domain which is divided into smaller parts to calculate and transfer data within the geometry. Sometimes it can feel as a trivial task, but is a very important factor in reaching good and stable solutions. To know the quality of the mesh, there are few indicators which are commonly used. They possess a significant impact on the stability and precision of numerical solution as described below.[18][19]

- **Orthogonal Quality:** It is computed for cells using the vector from the cell centroid to the centroid and faces of the adjacent cells. The worst cells are considered to have a orthogonal quality close to 0 while for the best cells, it is close to 1.
- **Skewness:** It determines how similar a cell or face is to that of ideal case (equilateral or equiangular). The worst cells are considered to have a skewness close to 1 while for the best cells, it is close to 0. Low orthogonal quality and high skewness are not recommended.
- **Aspect Ratio:** It defines how much a cell is stretched from its original position. It is recommended to avoid a big change in aspect ratio where there is a significant gradient in flow field.

Tetrahedral and hexagonal cell geometries are the most common base cells used in meshing. Depending on the complexity of the real geometry and the flows, it is a good practice to know which one to use. There are also cases where there is a transition between the two type of cells, which require prism or pyramids to preserve connection between nodes.

The geometry in this project is simple and mainly there are two direction in the main flow, perpendicular to each other. Hexagonal cells are best practiced when used in alignment with the main flow, which is possible in this case. Thus, the mesh will be dominated by hexagonal cells with a few exceptions to merge the two pipes together. The advantages of using hexagonal cells for simple cases are less amount of cells in the domain, less numerical diffusion and more accurate calculation, meaning less time needed to reach convergence. With circular geometries, the cells don't fit very well unless there is stretching on the cells which is preferably avoided to keep a good quality in the mesh. Thus, there is a specific layout for hexagonal cells which is employed for circular shapes, called Ogrid which is used in this project.

The O-grid is created by dividing the circular geometry into two parts. The center which will consist of a big square with very nicely shaped cells, while the outer part will have slightly stretched cells. Controlling the stretched cells can be done easily when using O-grid, so a good cell quality is kept throughout the whole circular area. Mesh pictures of the domain are presented below.

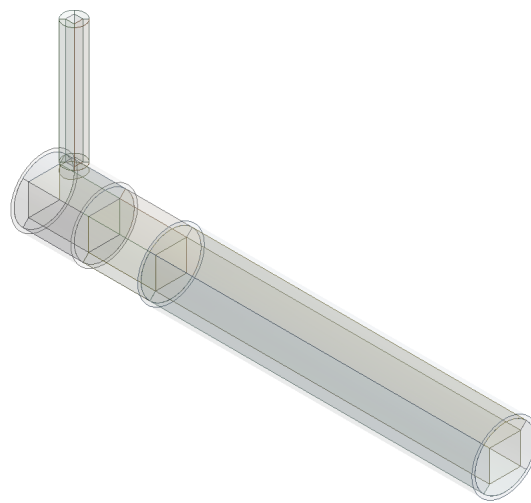


Figure 4.1: *Whole view of the domain*

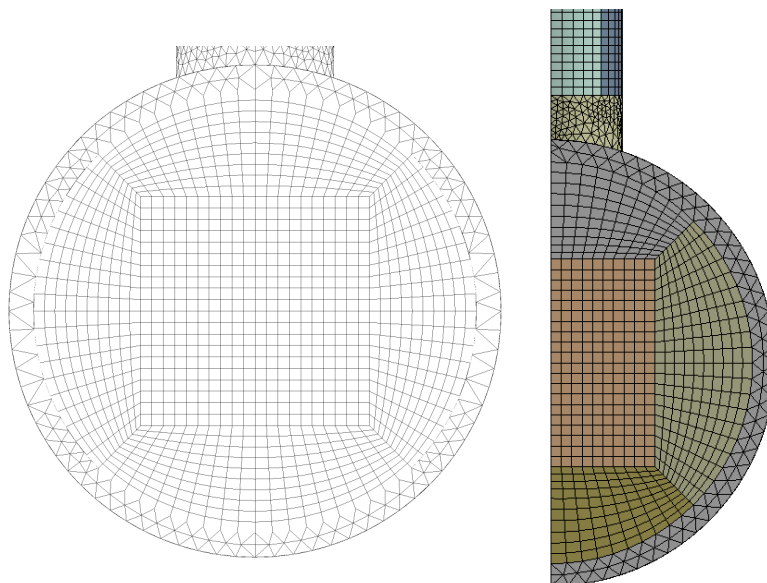


Figure 4.2: *O-grid meshing, more figures can be found in the Appendix*

4.3 Governing Transport Equations

In CFD modelling, conservation of mass, momentum, energy and species are the governing transport equations that are solved. In this section, these equations will be discussed in brief.

4.3.1 The equation of Continuity

The continuity equation describes the conservation of mass. The basic equation for continuity is:[6]

$$\text{Accumulation} = \frac{\text{Transport}}{\text{in}} - \frac{\text{Transport}}{\text{out}}$$

The very general form of the governing equation for continuity is presented as follows.

$$\frac{\partial \rho}{\partial t} + (\nabla \cdot \rho U) = S_m \quad (4.1)$$

Here, ρ is the fluid density, t is the time and U is the velocity of the flow in a vector field. The divergence term $\nabla \cdot$ defines the difference of mass flow in and mass flow out in the system. The derivative term defines the accumulation of mass in the system. Moreover, S_m is the source term, and it stands for the mass that has been added to the continuous phase from the dispersed phase. This mass conservation equation is valid for both compressible and incompressible fluid. [18] In fluent, this equation will be modified for special case such as incompressible flow of a Newtonian fluid.

4.3.2 The equation of Motion

The equation of motion describes the conservation of momentum and follows the momentum balance equation.[6]

$$\frac{\text{Rate of momentum accumulation}}{\text{Rate of momentum in}} = \frac{\text{Rate of momentum in}}{\text{Rate of momentum in}} - \frac{\text{Rate of momentum out}}{\text{Rate of momentum in}} + \frac{\text{Sum of forces acting on the system}}{\text{Rate of momentum in}}$$

The conservation of momentum is based on Newton's second law of motion. The general governing equation of motion is,

$$\frac{\partial(\rho \vec{U})}{\partial t} + \nabla \cdot (\rho \vec{U} \vec{U}) = -\nabla \cdot p + \nabla \cdot (\vec{\tau}) + \rho \vec{g} + \vec{F} \quad (4.2)$$

Here in this equation, \vec{U} stands for momentum, τ is the stress tensor and denotes the transported momentum into the system, $\rho \vec{g}$ and \vec{F} stands for gravitational and external body forces.[18]

4.3.3 The equation for energy transport

First and second law of thermodynamics are used to derive the energy transport equation in CFD. The conservation of energy says,[6]

$$\text{Total energy} = \text{Kinetic energy} + \text{Thermal energy} + \text{Chemical energy} + \text{Potential energy}$$

Using this formulation, the governing equation for energy transport for CFD programs can be presented as follows, which will also be modified in different cases.

$$\frac{\partial(\rho E)}{\partial t} + \nabla \cdot (\vec{U}(\rho E + p)) = -\nabla \cdot \left(\sum_j h_j J_j \right) + S_h \quad (4.3)$$

Here, J_j denotes the diffusion flux of species j , h is the enthalpy and S_h is the heat from any sources defined such as heat of chemical reaction. [18]

4.4 Numerical solvers

There are three methods to solve the above described governing equations. Finite Difference Methods (FDM), Finite Element Methods (FEM) and Finite Volume Methods (FVM). In both FEM and FVM, the flow domain is divided into small cells or volumes. These two are suitable to solve complex geometries. FDM method is suitable for simple regular shaped domains.

In Ansys Fluent, there are two kind of flow solver for considering the numerical schemes. Pressure based and Density based solver. In Pressure based solver, pressure field is extracted by solving pressure correction equation. It is obtained by manipulating continuity and momentum equations. This solver is used for low-speed (<0.3 Mach) incompressible flow. For compressible and high-speed flow, density based flow solver are used as a rule of thumb.[18]

4.4.1 Upwind schemes

The transport of data between cells is through numerical schemes, which estimates the next coming cell face value by extrapolating or interpolating data in adjacent cell centres. In first or second order upwind scheme, the transport of data is only done in the upstream of the flow direction. There are many other numerical schemes, but only the upwind ones are used in this project.[18]

First-order upwind is a simple and robust numerical scheme where the next cell face is decided from only the previous cell. It uses the approximation that the face value is equal to cell value in the upstream. First-order upwind scheme is not as commonly used as a final numerical scheme, due to numerical diffusion which causes an overestimation of entities when transporting data diagonally to the flow.[18]

Second-order upwind is more accurate than the first-order, but requires with longer computational time. The main difference between the two schemes is that the second order need both the upstream cell value and gradient to compute the next face value. A major setback is that second-order upwind is unbounded, meaning that it can cause stability issues when simulating such as divergence.[18]

4.5 Turbulence modeling

Quoting from Hinze, Turbulence can be defined as follows:

“Turbulent fluid motion is an irregular condition of flow in which the various quantities show random variation with time and space coordinates, so that statistically distinct average values can be discerned.”[20]

Turbulence is a irregular, random and chaotic state of the flow. It affects significantly the heat and mass transfer rate of the flow. Reynolds number is one of the parameter, a ratio between inertia force and viscous force, shows whether a flow is laminar or turbulent. A high Reynolds number means inertia force is significant compared to the viscous force, indicates the turbulent characteristics of the flow. Modeling the turbulence of a flow is a crucial part of solving CFD related problems as it has a great impact on the inter-phases.

Turbulence occurs when there are fluctuations in the flow field characterized by velocity fluctuations. These velocity fluctuations involve the mixing of transported quantities such as energy, momentum, species concentrations etc, which fluctuate as well in small scales and higher frequency. Since, simulating these small scale fluctuations are expensive in engineering calculations, various averaging techniques such as time, volume or ensemble averaging are applied or else manipulating the governing equations are used to remove these small scales resolutions. Performing these techniques will result in a modified sets of equations which contain additional variables to solve, but it reduces the cost of computational calculations while easing the effort. Thus a turbulence model will be needed to establish solving these additional variables.

The Reynolds Averaged Navier-Stokes (RANS) are equations of motion for turbulent fluid flow in a time averaging technique. It is an approach to describe the turbulent fluid flow by governing the transport of averaged flow quantities instead of instantaneous. It ignores small scale turbulent velocity fluctuations and

thus describe the turbulence in a time averaging method. The Navier-Stokes equations describe the fluid flow by assuming that fluid is continuum instead of discrete. But there are velocity fluctuations which needed to be modelled for the purpose of solving this equations. In order to decompose the Navier-Stokes equations to model those velocity fluctuations, an assumption has been made which is called Reynolds decomposition. It has assumed that time dependent velocity fluctuations can be isolated from the mean flow velocity. But this assumption has introduced a set of unknowns called Reynolds stresses, which are the functions of velocity fluctuations. Thus a turbulence model is needed to solve these unknowns and model the turbulent flow.[18]

In ANSYS Fluent, there are many turbulence models available. For example, Spalart Allmaras Model, k-epsilon Model, k-omega Model, Transition Shear Stress Transport (SST) model, Reynolds Stress Model (RSM), Detached Eddy Simulation (DES) Model and Large Eddy Simulation (LES) Model. In our project, the k-epsilon model was chosen for the following purposes.

Among the above stated turbulent models, the k- ϵ model is the most widely used turbulence model in industrial CFD. The k- ϵ model stores the turbulence kinetic energy and dissipation rate in each computational node, hence the name k-epsilon, where k stands for turbulence kinetic energy and ϵ stands for dissipation rate [21]. For this specific model, there are three options, a standard and two modified versions named RNG k- ϵ and Realizable k- ϵ model. For cases where flow feature big changes in streamline curvature or swirls, it has been proven that the modified versions show improved results compared to the standard one. Furthermore, the modification in realizable k- ϵ lies in the dissipation term and was created to battle the anomaly of round jet. Therefore, the setup of this model will be using the k- ϵ model for turbulence modeling of the flow. [18]

4.5.1 Transport equation for Turbulent Kinetic Energy, k

Among the three k- ϵ model, the k equation is same in all the three model. While deriving the transport equations for the k- ϵ model, the principal assumptions are that the flow has to be fully turbulent and molecular viscosity is negligible.

$$\frac{\partial(\rho.k)}{\partial t} + \frac{\partial(\rho.k.u_i)}{\partial x_i} = \frac{\partial[(\mu + \frac{\mu_t}{\sigma_\epsilon}) \cdot \frac{\partial k}{\partial x_j}]}{\partial x_j} + G_k + G_b + \rho.\epsilon - Y_M + S_k \quad (4.4)$$

4.5.2 Dissipation of Turbulent Kinetic Energy, ϵ

The dissipation term is different in different k- ϵ model. In standard k- ϵ model, the dissipation equation is,

$$\frac{\partial(\rho.\epsilon)}{\partial t} + \frac{\partial(\rho.\epsilon.u_i)}{\partial x_i} = \frac{\partial[(\mu + \frac{\mu_t}{\sigma_\epsilon}) \cdot \frac{\partial \epsilon}{\partial x_j}]}{\partial x_j} + C_{1\epsilon} \cdot \frac{\epsilon}{k} \cdot (G_k + C_{3\epsilon} \cdot G_b) - C_{2\epsilon} \cdot \rho \cdot \frac{\epsilon^2}{k} + S_\epsilon \quad (4.5)$$

Whereas for Realizable k- ϵ model, the dissipation term can be modelled as follows.

$$\frac{\partial(\rho.\epsilon)}{\partial t} + \frac{\partial(\rho.\epsilon.u_j)}{\partial x_j} = \frac{\partial[(\mu + \frac{\mu_t}{\sigma_\epsilon}) \cdot \frac{\partial \epsilon}{\partial x_j}]}{\partial x_j} + \rho C_{1\epsilon} S_\epsilon - \rho C_{2\epsilon} \frac{\epsilon^2}{k + \sqrt{\nu \epsilon}} + C_{1\epsilon} \cdot \frac{\epsilon}{k} \cdot C_{3\epsilon} \cdot G_b + S_\epsilon \quad (4.6)$$

Realizable model takes care of the turbulent viscosity by solving mathematical constraints of Reynolds stresses. In these above described equations, G_k and G_b is the turbulent kinetic energy due to mean velocity gradient and buoyancy. Y_M is the fluctuating dilation for compressible turbulence to overall dissipation rate, σ is the turbulent prandtl number for k and ϵ . S_k and S_ϵ are the source term. Finally, C_1 (varies in realizable k- ϵ), C_2 and $C_{1\epsilon}$ are model constants.

4.6 Modelling the Near-Wall Region

Modelling the wall is a very important step of CFD modelling, as turbulent flows are greatly affected by the different layers of the solid wall. There are two approach to model the near-wall region. The first approach is called the Wall Function Approach, where viscosity affected region is not be resolved, hence wall functions are

used to connect between near wall region and fully turbulent region. The other approach is called Near-Wall Model Approach, where viscosity affected region is resolved with a mesh all the way down to the wall. In high Reynolds number flow, the solution variable changes quickly in viscosity affected near wall region which does not need to be resolved. Therefore, wall functions are chosen as they are more economical and saves a lot of computational time. But in low Reynolds number flow, near wall modelling approach is a better choice as it is valid all the way to the wall by the modifications of turbulence modelling.

Commonly for many wall-functions, there is a requirement of keeping a Y^+ value within a certain range. The Y^+ value is a dimensionless measurement for the distance between the wall and the first computational layer and is defined as:

$$Y^+ \equiv \frac{u_* y}{\nu} \quad (4.7)$$

where u_* being the friction velocity, ν the kinematic viscosity and y is the distance from wall.

Due to the complexity in computing the viscous sublayer close to walls with similar to laminar behaviour, one would like to avoid this by having the first computational layer to be sufficiently distanced from the wall and only solve for the buffer/blending and fully turbulent layers. The main idea of having wall functions is to apply boundary conditions a few distance away from the wall so that the turbulence modelling can be solved. The main types of wall functions available in ANSYS Fluent are described below.

The default wall function in ANSYS Fluent is Standard Wall Functions where the wall Y^+ ranges between 30 to 100. It is used in high Reynolds number and wall bounded flows. But when there is a large pressure gradient in the wall, Non Equilibrium Wall Functions are used instead of Standard Wall Functions. The non-equilibrium wall function is preferred instead of the standard wall-function when there are complex flows such as separation, reattachment or other rapid changes in the mean flow. However, one of the limitations of non-equilibrium wall model is when the flow enters into a small channel. In this case, it is not certain if the monolith is causing inaccuracies, hence two wall models will also be considered. The Enhanced Wall Treatment, know as EWT is a two-layered model, which is able to resolve down to the viscous sublayer with the enhanced wall model, which occurs when $Y^+ \approx 1$. Since Y^+ may vary across the mesh, it can be difficult to restrict the value to 1 everywhere, thus comes the two layer approach. The two layered wall function means that the Enhanced Wall Function will be used for the appropriate Y^+ and for higher values, it will use standard wall function instead which is more suitable for $30 < Y^+ < 100$. The two layer approach gives the option to have a Y^+ insensitive wall treatment. The Scalable Wall Functions can be applied in very fine meshes. It is used when the Y^+ is below 11. This wall function avoids the collapse of Standard Wall functions. It is identical to Standard Wall Functions where Y^+ is more than 11.[18]

In our CFD modelling, Standard Wall Functions was chosen as the Reynolds number was moderately high and there were neither massive pressure gradients nor strong body forces in the wall present. Furthermore, the Y^+ fits the range of Standard wall function, meaning the other more insensitive models were not needed.

4.7 Turbulence quantities

As a turbulent flow is entering through the inlet or outlet of the system, it requires the specification of the transported turbulence quantities such as turbulence intensity, turbulent viscosity ratio, hydraulic diameter, and turbulence length scale. The impact of the turbulence parameters are most of the times very small and as long as they are set within a physical range, it should not affect the results too much. Thus, it is also a reasonable assumption to use uniform constant values, for the turbulence quantities, instead of being dependent on the velocity profile. In FLUENT, there are options to only define two of the turbulence quantities. The decision on which option to choose should be based on the flow types.[19]

- Intensity and Hydraulic Diameter, when there is a fully-developed internal flows.
- Intensity and Hydraulic Diameter, for flows downstream of turning vanes, perforated plates.
- Intensity and Length Scale for flows, bound to walls and the inlet involve a turbulent layer.

The turbulence quantities are used in FLUENT to estimate the values used in the turbulence models. Such as k and ϵ . Depending on which above options are used, FLUENT will treat and calculate the values accordingly.

4.7.1 Turbulence intensity

The definition of turbulence intensity is the root mean squared of the velocity fluctuations divided by the mean flow velocity. For fully developed internal flows, the turbulence intensity can be calculated as following.

$$I \equiv \frac{u'}{u_{avg}} = 0.16(Re_{DH})^{-\frac{1}{8}} \quad (4.8)$$

where Re_{DH} is the Reynolds number of the flow.[19]

The common range for turbulence intensity inside internal flows can range from $I < 1$ to $I = 5$ depending on the whether it is under-developed or fully developed flow. For a under-developed and undisturbed flow such as the inlet, one can set it closer to the lower bound.

4.7.2 Turbulence length scale

The turbulent length scale is the actual size of a large eddy. Since the eddy itself, can not be larger than the duct. Thus, there is a approximation for the turbulence length scale with respect to the duct size. $l = 0.07L$, where L is the hydraulic diameter of the duct. [19]

4.8 Modelling of the monolith

In fluent there is no option to set a certain body as a monolith with number of channels. Instead, the monolith treated as a porous media and is modeled with the use of viscous resistance parameters (inverse absolute permeability) in each direction given in unit $[1/m^2]$. This means, for a higher resistance value, the harder for the fluid to flow in that certain direction. To enable this option, one has to set the body as a porous zone, hence a porosity factor must be defined. The porosity can be set as the open frontal area, which is the fraction of open channels on the surface of the honeycomb.

The porosity can be calculated algebraically given the monolith properties are known. The monolith used in this project is 400/4, which means 400 cpsi and 4 mil. The definition of cpsi is cells per square inch and can be used to define a repeated distance s .

$$s = \sqrt{\frac{1}{N}} \quad (4.9)$$

where N is the number of channels per unit of cross-sectional area. Mil stands for milli inch of wall thickness. The open frontal area in one cell can thus be calculated.

$$OFA = \left(1 - \frac{w}{s}\right)^2 \quad (4.10)$$

where w is the wall thickness.[5]

The resistance parameters in tangential direction to the monolith channels will be set as a very high number to prevent momentum transport between channels. Literature suggests a value with three order of magnitude larger than the axial direction[22]. The axial direction will be a used as a tuning parameter to control the computed pressure drop and to match the ones measured from experiments. As a good starting point, the axial resistance should be modeled after a empirical expression found in an article about pressure drop for various catalytic converters. For the laminar flow inside the monolith channels, the pressure drop can be described with the Hagen-Poiseuille equation. Furthermore, it can be combined with the effects of kinetic energy from in the incoming gas in the inlet and outlet of the channel with a contribution factor, resulting in the following equation.

$$\Delta P = \frac{A \cdot \mu \cdot v \cdot L}{d_h^2} + \frac{B}{2} \cdot \rho \cdot v^2 \quad (4.11)$$

where $A=28.4$, is a parameter of channel shape and $B=0.41$ is a contribution factor from the second term in equation (11.2). A and B are experimentally determined in the Ekström-papers.[23]

4.9 Space velocity

Space velocity is the common flow unit used in combustion emission technology. It is given in the unit [h^{-1}] and the ratio of Volumetric flow rate, at standard temperature and pressure, and the reactor volume.[24] A good feature when using space velocity is the independency of temperature. It is well known that the exhaust gas temperatures are significantly hotter than normal air. Therefore, it is more convenient to use space velocity rather than velocity which is a flow rate which changes significantly depending on the temperature. However, since the space velocity is mostly used only in combustion terms, a transition is needed for the simulations.

$$Space\ Velocity = \frac{\dot{V}_{STP}}{V_{reactor}} \quad (4.12)$$

where \dot{V}_{STP} is the volumetric flow rate in standard temperature and pressure and $V_{reactor}$ is the catalyst bed volume.

4.9.1 Space velocity into Velocity

The transition from space velocity to velocity is fairly simple. Since the molar flow is unchanged, the ideal gas law can be used to determine the molar flow given standard temperature and pressure.

$$n = \frac{P\dot{V}}{RT} = \frac{P_s\dot{V}_{STP}}{RT_s} \rightarrow \frac{P_s}{P} \cdot \frac{T}{T_s} \cdot \dot{V}_{STP} = \dot{V} \quad (4.13)$$

where P_s and T_s are standard pressure and temperature.

Finally, with the volumetric flow, the velocity can be calculated.

$$v = \frac{Volumetric\ flow\ rate(\dot{V})}{Cross-sectional\ Area} \quad (4.14)$$

As shown in the above expression, it is easy to see that velocity is proportional to the volumetric flow. Thus, it is not a good representation for fixed space velocity in simulations, since it is dependent on temperature.

4.9.2 Space velocity into Mass flow

Mass flow is the product of volumetric flow and density, which can follow the same calculation as in velocity. Continuing from the volumetric flow in equation (4.13), the remaining step is to simply multiply with density.

$$\dot{m} = \rho \cdot \dot{V} = \frac{PM_w}{RT} \cdot \frac{\dot{n}RT}{P} = M_w \cdot \dot{n} \quad (4.15)$$

where M_w is the molar mass and \dot{n} is the molar flow rate.

Since neither molar flow rate nor molar mass is temperature dependent, mass flow is a good input variable to represent the space velocity.

The relation between mass flow and space velocity can be shown by combining equations (4.12), (4.13) and (4.15).

$$Space\ velocity = \dot{m} \left(\frac{RT_s}{M_w P_s} \cdot \frac{1}{V_{reactor}} \right) = \dot{m} \cdot Constant \quad (4.16)$$

This concludes the proportionality between space velocity and mass flow, which is now proven to be the better representation for space velocity compared to velocity.

4.10 Simulation

The final model will be a transient simulation with two changing variables in the reactor in 3D. However, the model will be developed gradually from an initial simple steady-state 2D simulation, due to the unstable nature of diving directly into a complex model. Taking one step at a time is easier to keep track of what factor causes a non-converging solution. The idea is to get a 3D steady state model, with all relevant physics included. The same physics will hence be implemented into a 3D transient simulation. Temperature and flow will be taken care of, one at a time, in a one variable simulation until both are converged. When stability is achieved for respective variable in transient simulation, the final simulation of two transient variables will be developed, which will be the final model.

4.10.1 Convergence

In computational fluid dynamics (CFD), convergence is essential. The exact solution is most of the times unknown and the calculated value should be approaching a final value in a iterative procedure. The general way to depict convergence is to monitor the Residual root mean square (RMS) for the equations solved, such as momentum or energy etc.[19] However, keep in mind the residuals are showing a fraction between the starting and current residual for each iteration and can in specific cases be insufficient in defining convergence. Such a case can be, when the initialization is nowhere close to the real value, resulting in a very large first residual which can decrease in several magnitudes in very few iterations. Same goes for a very good starting point, which can be converged even with relatively large residuals. For this reason, it is recommended to also monitor any relevant physical property in the system and make sure they are stable in the converged solution.

4.10.2 Residuals

The default tolerance of scaled residual RMS in fluent is $1e - 03$ except for the energy equation, which is set to $1e - 06$. The solver declares the solution as converged when all variables have decreased below the tolerance limits and stops the calculation. For scaled residuals, good starting value for continuity can cause the initial residual to be very small, resulting in large scaled residual further in the calculations. There is also an option to monitor unscaled residuals with the same tolerance. A good initial guess will result in big residuals and bad initial guess can result in small residuals with falsely converged solution. Since there is no universal tolerance value which is appropriate for all classes of problems, it is even more important to monitor other quantities of interest.

4.10.3 Under-relaxation factor (URF)

Under-relaxation factor is used for pressure-based solver to stabilize the iterative step by controlling the update of variables.[19] URF is a value ranging from 0 to 1, which controls how much of the previous value of a variable will be affecting the updated value. For URF=1, the updated value is not affected by the previous value. Optimally, one should aim to have high URF for faster convergence. For cases where the final solution is oscillating, one possible cause could be due to a too aggressive solver. Thus, by decreasing the under-relaxation factor, one can reduce the overshoot and stabilize the solution.

4.10.4 Grid independence

Once a simulation model is solved and converged with appropriate residuals and the relevant quantities are stable, it is also important to keep in mind that the solution is based on the mathematical problem provided by the mesh and implemented physics and respective closures[19]. Thus, to check the validity of a simulation model, the grid has to be tested. A grid independent solution is achieved when a refined mesh shows similar results as the coarser mesh. Hence, the mesh is proven to contain small enough cells to accurately reproduce the solution of an infinitely fine mesh. A general rule of thumb is to have a tolerance of 5 to 10% deviation between two mesh cases.[18]

5 Theory: D-Optimal Design

In this chapter, a brief description of the statistical methods and tools for D-optimal study, which were used in the project, will be discussed.

5.1 Principal component analysis(PCA)

Principal component analysis is a statistical mathematical procedure commonly used when handling large data sets with high dimensions. The purpose of this tool is to reduce the number of dimensions to simplify the processing on the data, while retaining the information needed by creating a model to represent the data. The analysis is carried out by constructing principal components(PC), which are orthogonal transformations of a set in the observations. Due to the orthogonal nature in PC, the set of values in each PC is linearly uncorrelated, even if the true data is highly correlated. The first principal component is constructed such that it has the highest possible variance, which means it will account for the majority of the variability in the data. A second principal component will thus be constructed in the same manner with a restriction of being orthogonal to any other previous ones. In this manner, the first component will always be the most important to express the data, while additional components can be a good complement to retain valuable information by increasing the dimension of the model.[25]

5.2 Unit-variance scaling

Unit variance scaling is commonly used in processing data where there is a big range of values. It is convenient to scale the data with mean value as zero, so that the minimal and maximal values are more similar but in opposite directions. Thus, in modelling, both the minimum and maximum data can contribute to the analysis equally. Unit variance scaling uses the zero as mean and divides it by the standard deviation, following the formula below:

$$X_{i,scaled} = \frac{X_i - \bar{X}}{\sigma} \quad (5.1)$$

where X_i can be either a row or a column.

5.3 D-optimal design in MATLAB

The D-optimal design is a search algorithm which uses iterative method to find the optimal set of candidates. The optimal set in D-optimal design, is the set with minimal covariance in the parameters for the model, which can also be described as largest determinant of $[X'X]$, where X is a row. In MATLAB, there are multiple tools to generate the D-optimal design, but the tool which is used in this project is candidate exchange. The candidate exchange algorithm selects a random row as a starting point and uses an iterative procedure to find better candidates by replacing the current with randomly selected rows, from the model matrix, where $\det[X'X]$ is larger.[26]

6 Setting up a simulation

In previous chapter, the turbulence and near wall model were thoroughly described. In this chapter, the steps on finding the missing parameters to complete the initial CFD model is described.

6.1 Initial conditions

Since the initial model was developed before performing any laboratory experiments, it was not decided on what temperatures and inlet velocities would be present in the system. Thus, arbitrary values with relevant ranges were to be used in the initial simulation. It was earlier mentioned that space velocity in EATS generally has a range from 60 000 to 150 000 [h^{-1}], which corresponds to a certain velocity in the outlet depending on the temperature. However, since the model would later be tested in comparison to laboratory experiments, it was uncertain if the same space velocity could be reached with the current equipment. Thus, the aim was to set it closer to the lower bounds, where inlet-mass flow was set to 0.01[kg/s] at 571K, which is equivalent to 51 300 [h^{-1}] with an actual heating effect of 2.5kW.

6.2 Turbulence quantities

From previous chapter, it was mentioned there are different approach in FLUENT to which turbulence quantities are needed, depending on the flow conditions. In this project, there will only be internal flows, where the inlet pipe will have a fully developed flow before entering the reactor. Hence, the defined turbulence quantities will be turbulence intensity and hydraulic diameter.

6.3 Boundary Conditions

On the walls, heat transport will be present with a free convection with an arbitrary heat transport coefficient taken from literature. For the momentum equation, no slip condition will be used.

Outlet will be set as an outflow, which is a good option when the pressure and flow velocity is unknown prior to simulating the solution. Optimally, the velocity profile should be fully developed before reaching the exit, however that is something to be verified in the results.[19]

The heat transport in the monolith part of the reactor is insulated with glass wool, which is generally a material with low thermal conductivity. In order to account for heat transport through the insulation onto the steel wall and further into convection, a two-shell convection option was used in FLUENT for this specific area.

6.4 Incompressible ideal gas density

The density can be calculated through incompressible ideal gas law in FLUENT, which is a modification for the ideal gas law. The density will mainly be dependent temperature and less dependent on pressure, since the pressure will be pre-defined. Ideal gas law is a moderately accurate way to describe the gas expansion for a high range of temperatures, but not as accurate for increasing pressures.

The density in incompressible ideal gas law model is determined through the equation 6.1[19]:

$$\rho = \frac{P_{op}M_w}{RT} \quad (6.1)$$

where:

P_{op} = operating pressure

M_w = molecular weight

R = gas constant

T = temperature

According to International Standard Atmosphere (ISA), the density of air at sea level and 15°C is 1.225 kg/m³. A comparison between constant and incompressible ideal model is shown in figure 6.1 below.

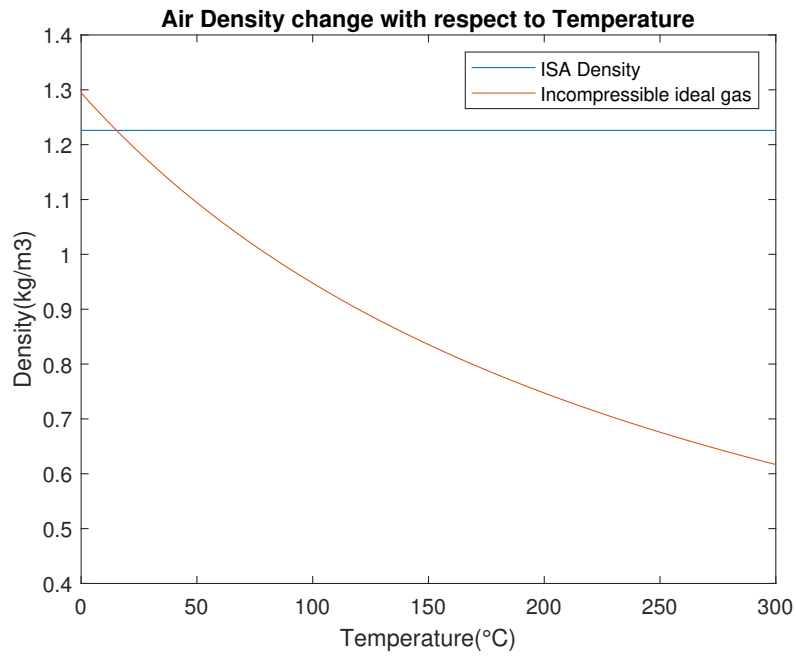


Figure 6.1: *Density with respect to temperature changes for operating pressure at 1 atmosphere.*

When the incompressible ideal gas law is used for density, a operating pressure has to be given, which was assumed to be close to 1 atm.

7 Experimental Methodology

In this chapter, the experimental limitations, arrangements and methodology will be described.

7.1 Preliminary experimental limits

The following graph describes the range of temperature with respect to the space velocity and volumetric flow rate for different heating power from the heater. As we have a heater with a highest capacity of 3kW, the highest temperature of the air that can be reached in our experiment is approximately 810°C at the lowest gas flow. When the gas flow increases, the temperature will decrease as the gas will have less residence time to heat up because of high velocity and vice versa.

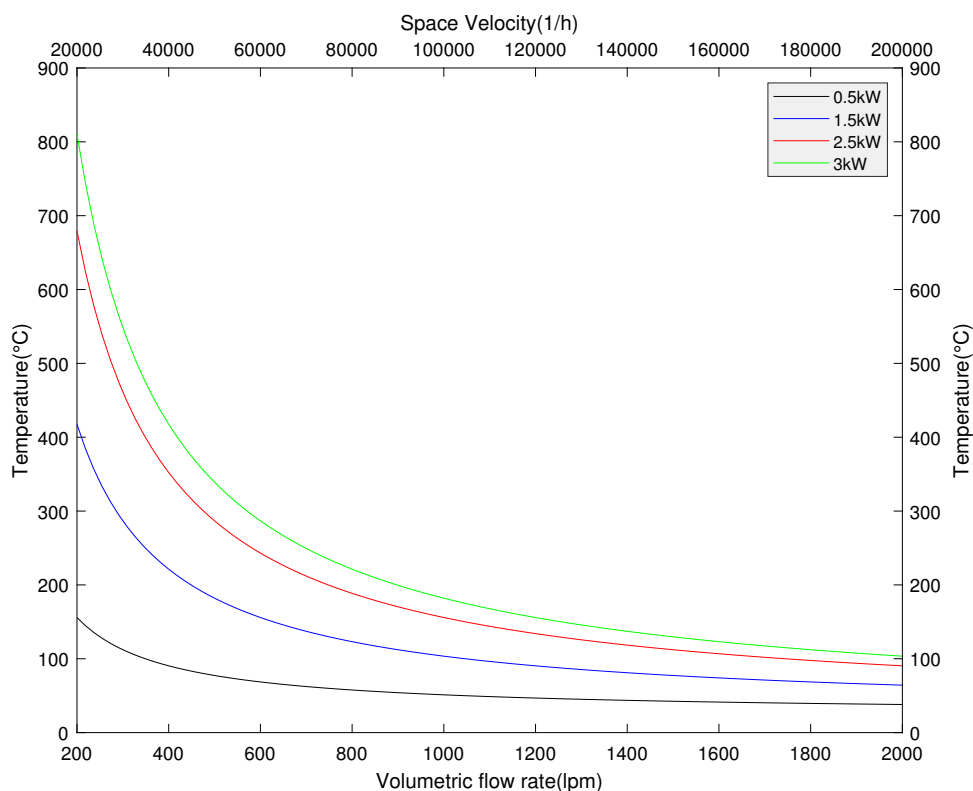


Figure 7.1: *Experimental temperature limitations depending on flow rate*

It can be seen that the range of the temperature is approximately 50°C to 810°C with respect to the space velocity range of 20 000 h^{-1} to 200 000 h^{-1} which corresponds to air volumetric flow rate of 200 lpm to 2000 lpm for different heating of 0.5 kW to 3 kW from the heater.

7.2 Experimental Setup

Three different experiments will be done for evaluation of flow behaviour in the outlet of the monolith. The goal is to identify temperature and velocity gradients in the monolith channels due to the bent pipe inlet. Detailed risk analysis of the laboratory experiment will be found on the Appendix section.

7.2.1 Experimental arrangement

The existing setup of the laboratory tent will be used for testing air flow inside a catalytic reactor with slight modifications. In this case, an extended pipe will be attached after the laminar air flow element,

where the heating of air will take place by a heater. The hot air (50°C to 810°C depending on the heat (maximum 3 kW) from heater) will pass through the monolith situated inside the catalytic reactor where fourteen thermocouples are attached at different locations to measure the temperature of the inlet and outlet of the monolith. Additionally, a fifteenth thermocouple is placed in the entrance of the reactor to observe the inlet temperature and also operating the the heater’s heating. The velocity at the different locations of monolith will be measured with a Prandtl tube at the outlet. Using the results from this experiment, the simulation results will be verified to conclude the final modeling of the EATS system.

7.2.2 Experimental flow chart

As per the experimental arrangement, the flow chart for the experiment is presented below. It shows the pressurized workshop air will be regulated by a pressure regulator to control the inflow. The flow will then pass through the laminar air flow element and a heater is placed after that. The heater will heat the air flow to a desired temperature according to the experimental requirement. The hot air will then pass through the reactor via a bend pipe. A Prandtl tube will be used to capture the velocities of the air flow at different location of the monolith outlet. The air flow leaving the reactor, will be freely let go to the surroundings as it is completely harmless and not excessively warm for any risk of fire.

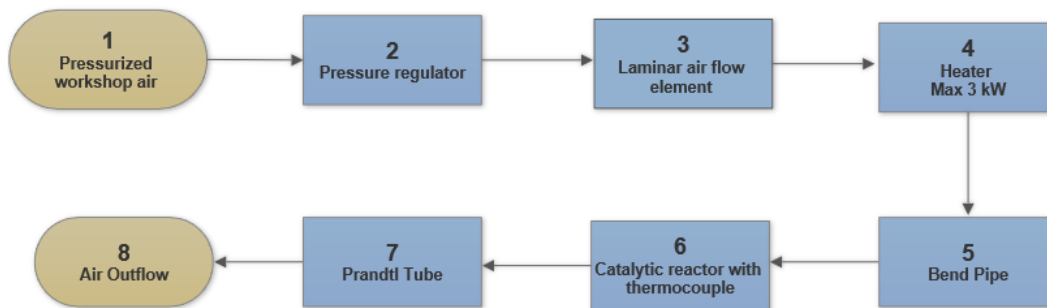


Figure 7.2: Experimental flow chart

7.2.3 Images of Equipment

The images shown below are taken from the laboratory and the equipment used in the experiment are shown in a sequential order of experimental arrangement and flowchart.



Figure 7.3: Equipment used in the experiment in a sequential order

7.2.4 Functions of the equipment

The functions of the equipment used in the experiment are listed in the table below.

Table 7.1: Experimental equipment's activity

Equipment/Activity	Function
1. Pressurized workshop air	Directs the air flow towards the reactor
2. Pressure regulator	Regulates the pressure to control mass flow in the inlet
3. Laminar air flow element	Measures the mass flow with the help of pressure drop
4. Heater	Heats the air to a desired temperature
5. Bend pipe	Bends the air flow into the reactor
6. Catalytic reactor with thermocouple	Hot air flow goes inside the reactor with a bend, the monolith is attached with 14 thermocouples to measure the temperature at different location
7. Prandtl tube	Measures the flow of the outlet air
8. Air outflow	Hot outlet air leaves the reactor to the surroundings

7.2.5 Laboratory view

The whole view of the laboratory arrangement are shown below. The photo was taken from a view so it can show the overall view of the experiment.

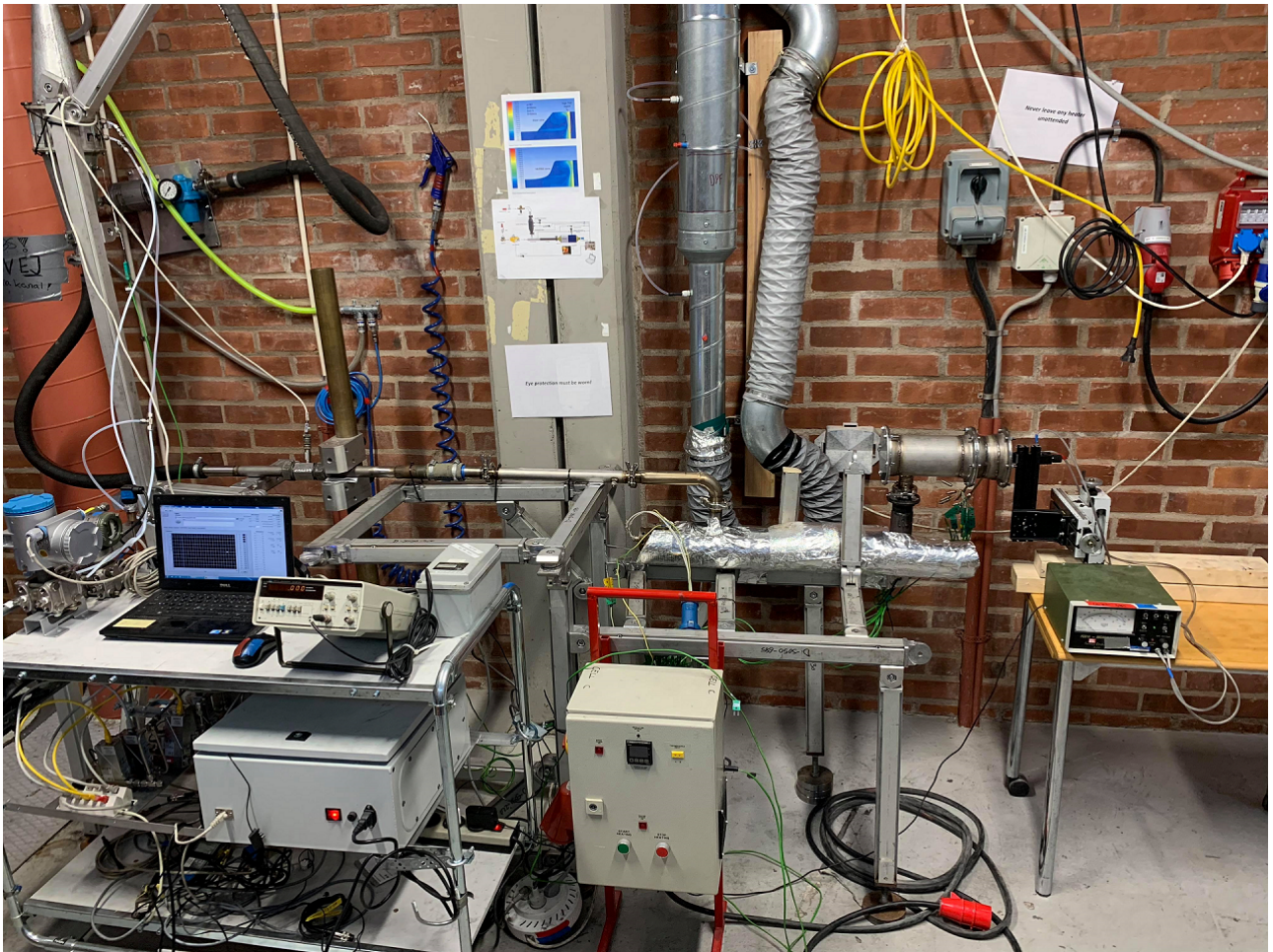


Figure 7.4: *The overall view of the experimental setup in the laboratory*

7.2.6 Position of Thermocouples

Thermocouples are inserted into the monolith from the outlet. The picture presented here is a view of the outlet side of the monolith. The numbers 1 to 15 and orange colored X represent the thermocouple numbers and their positions respectively. U, R, D, L represent the locations up, right, down and left. The thermocouples are installed only on one side assuming that the monolith is vertically symmetric. Thermocouples were being avoided to be put along the middle part (U to D line) to promote an undisturbed flow in there and for the simplicity of measuring the outlet air flow with Prandtl tube.

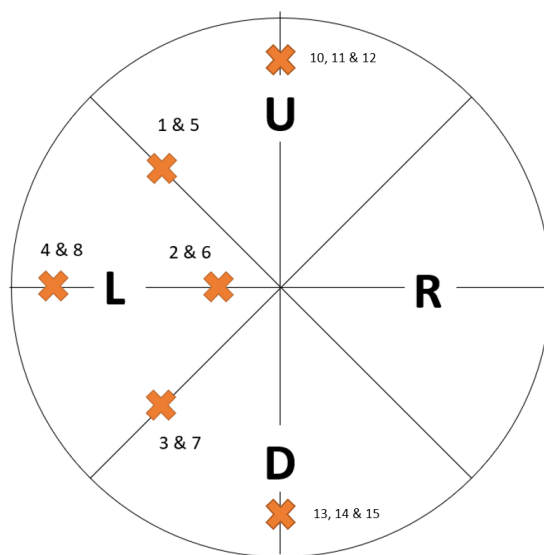


Figure 7.5: Position of thermocouples in the monolith of the reactor

1, 2, 3, 4: 1-2 cm into monolith from outlet, these four thermocouples will measure the temperature in the outlet part of the monolith.

5, 6, 7, 8: 7-8 cm into monolith from outlet, these four thermocouples will measure the temperature in the inlet part of the monolith.

9 : This thermocouple (not shown as its in the reactor inlet) will be in the reactor inlet to control the heater and observing reactor inlet temperature.

10, 13: 1 cm before the monolith inlet at U and D position respectively.

11, 12: In the U part of monolith inlet and outlet respectively.

14, 15: In the D part of monolith inlet and outlet respectively.

Table 7.2: Thermocouple positions

Inlet	Outlet
5	1
6	2
7	3
8	4
11	12
14	15

7.3 Experimental procedure

Procedures for the three experiments conducted in this above described arrangement, are as follows.

7.3.1 Experiment 1: Observation of velocity profiles

The first experiment was done to observe the velocity profile of the exhaust gas flow inside the monolith at ambient or room temperature. The velocities in different position of the monolith outlet was captured by a prandtl tube at three different flow conditions; low, medium and high flow. As the monolith was assumed to be vertically symmetric and the left side of it has thermocouple inserted, the right side was used by prandtl tube to capture the velocity profile, where the locations are showed as U, R and D in 7.5. Corresponding pressure and the frequency for the three different flow conditions are shown in the following table.

Table 7.3: Experimental conditions used in the laboratory

Flow condition	Volumetric flow rate (lpm)	Pressure (bar)	Frequency (kHz)
Low	200	0.75	0.164
Medium	400	2	0.316
High	700	4	0.526

7.3.2 Experiment 2: Testing of proposed flow conditions

The volumetric flow rate will be regulated in a manner that it can follow a protocol of a specific flow condition which will reflect the space velocity of the exhaust gas to the time. The protocol will be followed in five sections of the flow described as follows. The experimental testing duration will be restricted to 120 seconds in total.

- Low flow: 0-20 s
- Medium flow: 20-40 s
- Low flow: 40-70 s
- High flow: 70-100 s
- Low flow: 100-120 s

The following picture represents these flow conditions described above for the given catalyst volume of 0.6 l.

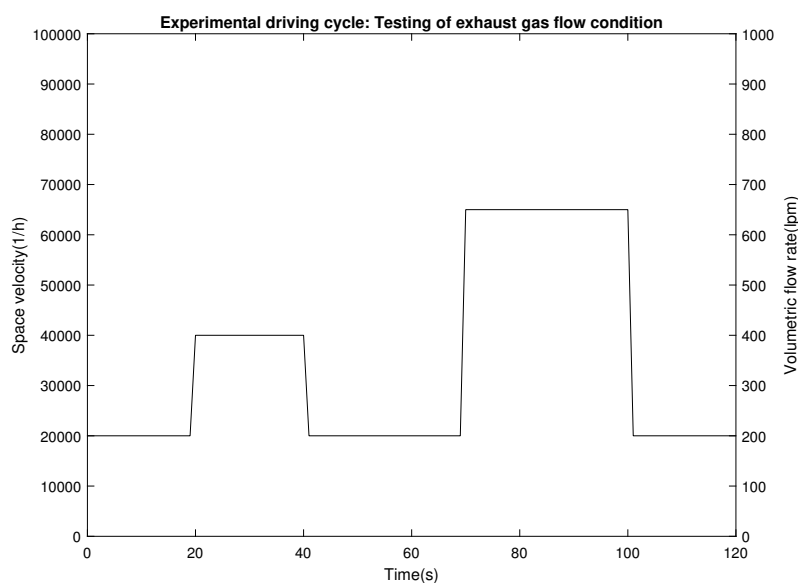


Figure 7.6: Five flow conditions of exhaust gas

The flow profile depicted above is initially tested without heating at room temperature (20°C), but the thermocouple will not show any readings as the test will be done in room temperature. Thereafter, the heater will be used to set the inlet temperature to 60°C and the same flow pattern will be tested again. Thus thermocouples will show readings and temperature profiles for this specific five flow conditions will be evaluated.

7.3.3 Experiment 3a: Reactor cooling in three flow conditions

The time for cooling down the reactor was tested by running three different flows (high, medium and low). All of the three flows were heated to 60°C and then the heater was turned off. The cooling effect in each of the three flows were observed till they reached 25°C. The flows were changed only when a steady state had been reached both in 60°C and 25°C.

Therefore, at first the flow was set to low flow condition at 25°C and then the heater was turned on. When the temperature of the gas stabilize at 60°C, the heater was turned of and let the flow cool down to 25°C. When the flow stabilize at 25°C, the flow was set to medium and high flow condition respectively and the same process was repeated again. The purpose for this experiment is to later adapt the CFD model to match the cooling in the real reactor.

7.3.4 Experiment 3b: Reactor cooling in two flow conditions

This was also a cooling experiment. This time the experiment was done in high and medium flow conditions with the highest heating capacity of the heater. No temperature limit was set in the heater and hence the temperature could reach according to the heater's highest capacity. In high and medium flow, the temperature of the flow reaches up to 220°C and 300°C respectively. The experiment was conducted to observe the cooling effect from the highest temperature in different flow conditions and the purpose was same as experiment 3a.

8 Adjusting The Model

Before doing the laboratory experiments, a model on a fictitious reactor is setup and simulated. Adjustments in the model will be made to minimize the deviation from the experimental values for an improved accuracy, including changes for initial conditions in the inlet, permeability for the monolith channels and heat transfer coefficients. The model is most likely to be changed when the xperimental data is gathered, for the model to be specifically describing the given reactor.

Steady-state data will be used to adjust the heat-loss across the reactor such that the sensors in simulation and experiment show a similar behaviour for each position. Additionally, a transient cooling simulation will be used to monitor the behaviour in changing flow temperatures according to experiment 3b.

9 Processing Temperature and Velocity sensor data

The sensor data which are collected from the 82 possible locations in the simulations are transposed so that all the rows represent every sensor location and every column is a set of data collected at a specific time. Note that for every specific time, there are two corresponding columns, due to one being temperature and the other velocity measurements.

The transposed data is then used in unit variance scaling for each column, see equation 5.1. The scaled data is thereafter, used in the PCA code in matlab, which creates a number of PC's. The PCs and the corresponding accuracies in the model can be extracted from the code. Finally, the principal component model is used in the D-optimal candidate exchange algorithm to find the optimal candidate set.

To make it possible to account for both velocity and temperature data in one model. It was decided to make the candidate exchange algorithm based on the heat flux, Q . Calculated as following:

$$Q_{tot} = cp \sum_{i=1}^{82} A_i \cdot v_i \cdot \rho_i \cdot (T_i - T_{ref}) \quad (9.1)$$

where i represents the sensor and A_i is the area of the which the sensor covers. However, since the data saved from FLUENT is based on the area-weighted average value of each specific point, it doesn't have an actual area. It is rather an interpolation with area as weighting of the nearby nodes inside the computational cell, in which the point is defined. To proceed further with the equation above, it was necessary to make an assumption for A_i , which for the sake of simplicity was determined as $A_{total}/82$, meaning each sensor covers equally big area.

In this project, the maximum desired number of sensors is 4. Thus, the least number of PC's needed to have four different locations is 3 PC's. However, the root mean square of the model will be observed, depending on number of components to reduce the error to reassure a good level of accuracy is achieved. Additionally, less PCs and sensors will presented so that a comparison in accuracy can be conducted.

A weighting factor will be introduced for the selected optimal locations by regression, with the same area assumption as before. Using only the data from optimal locations, the same equation for heat flux is calculated.

$$Q_s = cp \cdot A_s \cdot v_s \cdot \rho_s \cdot (T_s - T_{ref}) \quad (9.2)$$

where T_s and v_s are the data specifically for the optimal locations.

A unit variance scaling is conducted on both the Q_{tot} and Q_s according to equation (5.1). The general way to find the weight factor is to solve the equation from following.

$$Y = X/W \rightarrow W = (X'X)^{-1}(X'Y) \quad (9.3)$$

where X and Y represents the UV-scaled data of Q_s and Q_{tot} respectively.

Thus, the predicted value for Q_{tot} can be estimated by using the weighted model.

$$\hat{Y} = \bar{Y} + X \cdot W \quad (9.4)$$

where \hat{Y} is the prediction.

The accuracy of the model can thus be determined by observing the residuals, defined as defined as $Res = Y - \hat{Y}$.

10 Optimal Sensor Locations

D-Optimal is used to find the optimal sensor placements. The objective is to maximize the gain, using four sensors to determine the state of the reactor. To make this possible, a vast number of potential positions are created in FLUENT to collect temperature and velocity in each data point throughout a transient simulation. This data is later used in Principal component analysis to create a model, consisting of multiple principal components, which can be used in the D-Optimal algorithm in MATLAB.

The D-optimal design will be conducted on three different transient simulation cases. The first and second case will be the simulation of cooling effect with tuned parameters following the temperature profile in experiment 3 for medium and high flows respectively. The third case will be the transient profile of experiment 2, where the temperature profile is following experiment 2. In each case, the heat flux will be calculated for the average over the outlet and compared with a weighted model for four specific sensor locations. Thus, both velocity and temperature will be considered in the determination of sensor location.

Finally, a comparison of which locations are preferred in each case will show if the optimal location has been found for a general case.

11 Results and Discussions

In this chapter, the results and discussions for both simulation and experimental results will be shown.

11.1 Initial Simulation Model

The goal of the steady simulation is to first, confirm parameters such as pressure drop to match with literature according to equation (11.2). This is done by changing the inverse permeability, which generates a resistance in each direction to match the pressure drop over the monolith. Secondly, the stability of the model was studied so that it can be used for the transient simulation. Since the geometry and flow is not very complex in this case, the convergence was shown to be very smooth and no signs of fluctuations in residuals were found.

The steady simulation is also used to show the heat and flow distributions in the system for fixed velocity and temperature. The heat flux is governed by free convection due to temperature difference in the inlet gas and the surrounding air in room temperature. The heat transfer coefficient, h , is set to constant at $20(kW/m^2 \cdot k)$, which is close to the upper limit for gas convection according to literature. To account for insulation material between the pipe wall and monolith, a shell conduction model with two layers is used at the specific region. Due to many missing conditions needed to run the simulation, arbitrary values were approximated so that the behaviours in the model could be processed and observed.

As shown in figure 6.1, it is necessary to implement incompressible ideal gas law for increasing temperatures. When using the incompressible ideal gas model in FLUENT, the velocity becomes dependent on temperature. It accounts for the expansion of the gas when heated up. Therefore, it is more convenient to give the mass flow in the inlet, because it is proportional to space velocity and temperature independent. To find a suitable mass flow for the reactor, an arbitrary value for velocity was chosen with a fixed space velocity of $51\ 300\ h^{-1}$ which corresponds to approximately $0.01kg/s$.

Inlet temperature was calculated with a limitation in the heater, assuming only $2.5kW$ of the heat was transferred into the fluid with space velocity $51\ 300\ [h^{-1}]$, see figure 7.1. It can also be calculated through following equation:

$$q = \dot{m}c_p(T - T_{ref}) \rightarrow T = \frac{q}{\dot{m}c_p} + 298 = 571K \quad (11.1)$$

where:

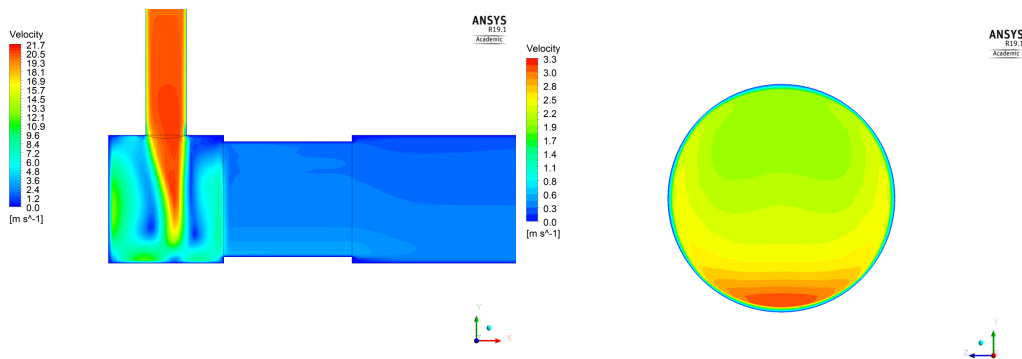
- \dot{m} = mass flow [kg/s]
- c_p = specific heat capacity [kJ/kg·K]
- T = temperature [K]
- T_{ref} = reference at 293 K ambient temperature

For a heater of $2.5kW$ with space velocity $51\ 300\ h^{-1}$, ambient air is expected to be heated up to $550K$ before entering through the inlet pipe.

Table 11.1: Summarized settings for the first model in FLUENT.

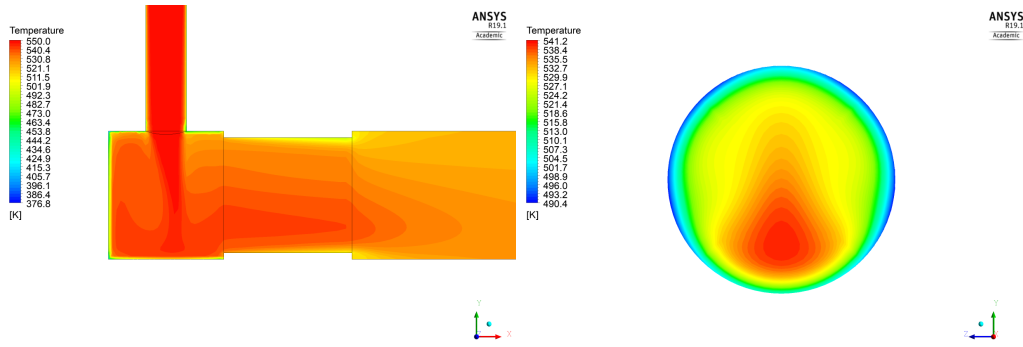
Models and Conditions	Turbulence model Boundary wall Near-wall model Inlet boundary cond. Outlet boundary cond. Wall boundary cond.	realizable k- ϵ No slip Standard wall function Mass flow-inlet Outflow Free convection at room temperature $h=20 [W/m^2 \cdot K]$
Settings	Mass flow Inlet temperature Inverse absolute permeability Porosity Operating pressure tolerance limit	0.0098 [kg/s] 550 [K] $1.625 \cdot 10^8$ in axial direction $2 \cdot 10^{12}$ in radial direction 83% 1 [atm] $1 \cdot 10^{-6}$
Air	Density Specific heat Thermal conductivity	Incompressible ideal gas 1.006 [kJ/kg] 0.0242 [W/m · K]
Insulation	Density Specific heat Thermal conductivity	380 [kg/m ³] Assumed air Assumed air
Cordierite	Density Specific heat Thermal conductivity	279 [kg/m ³] 1050 [kJ/kg] 1.8 [W/m · K] in axial direction 0.9 [W/m · K] in radial direction

The first model is simulated with the settings above. Since many of the parameters are approximated or taken arbitrarily, it is merely results to observe the behaviour in velocity and temperature distributions.



(a) Velocity distribution visualized in a plane view. (b) Velocity distribution in the monolith outlet.

Figure 11.1: The velocity distributions of the first model.



(a) Temperature distribution visualized in a plane view. (b) Temperature distribution in the monolith outlet.

Figure 11.2: The temperature distributions of the first model.

11.1.1 Pressure drop

Using the specifications of the catalytic converter of 400/4, the equation (4.9),(4.10) can be solved. However, the open frontal area is not affecting the flow in FLUENT, because it is a parameter for the the ratio of fluid and solid heat-transport properties. The resulting superficial velocity in the catalyst will hence be divided with OFA, which will be the real velocity.

Inverse permeability is used to manage the pressure drop of a real case. The pressure drop through a small square channel can be approximated by equation (11.2).

$$\Delta P = \frac{28.4\mu Lv}{d_h^2} + \frac{0.41}{2}\rho v^2 = 186.7Pa \quad (11.2)$$

where v is the velocity in a channel.

The pressure drop across the monolith section in the simulations can be visualized in CFD post. Since the pressure drop varies slightly due to non-uniform velocity distribution across the monolith, the compared value will be taken from the center of the reactor. The error between the calculated and simulated pressure drop is sufficiently small, which concludes an accurate simulated pressure drop and the corresponding inverse permeability in the axial direction.

11.1.2 Grid independence

A grid Independence validation was carried out by gradually decreasing the sizes of the cells in the mesh. Thus running the same setup of for every mesh case, the independence could be verified. The monitored variables are total mass flux, velocity magnitude and temperature contours in respective case. The setup used is the same as before and can be found in table 11.1.

The three different meshing cases approximately consist of 129 000, 234 000 and 1 030 000 cells respectively. It was shown in the comparison that no major differences were found among the three cases in both temperature and velocity distributions, which leads to the decision to use the 129 000 cells case in future simulations due to the cheaper computational cost. The figures for grid Independence can be found in the Appendix B B.2 and B.3.

11.2 Experiments

Results from all of the three experiments are presented below.

11.2.1 Experiment 1: Observation of velocity profiles

The velocities from the different locations of the monolith outlet by Prandtl tube are shown in the table below.

Table 11.2: Velocities of outlet air at the different location of monolith outlet face at three different flow conditions

Volumetric flow rate(lpm)	Center velocity (m/s)	Top velocity D (m/s)	Bottom Velocity U (m/s)	Side velocity R (m/s)
200	0.9	0.9	1	0.9
400	1.9	1.1	2	2
700	3	2	3.6	3.5

The table shows that highest velocities recorded is in the bottom part of the monolith outlet which is also true in the simulations. However, when comparing for other locations, it no longer looks as promising. The procedure to use a Prandtl tube to read the velocities was very difficult, due to the inability to completely control the distance between the outlet and tube. It was very important to be very close to the outlet to accurately read the velocities coming out from the monolith channels. However, it was also a risk to scrape or destroy the delicate cordierite walls, when going too close. Caution was taken not to harm the monolith and thus, it is probable that the velocity measurements were not taken completely correct.

11.2.2 Experiment 2: Testing of proposed flow conditions

According to the five flow conditions described in the methodology, the comparison of planned and experimental flow condition are shown below. The experimental flow condition is pretty similar to that of the planned, but with a small deviation because of the regulating error of the pressure regulator.

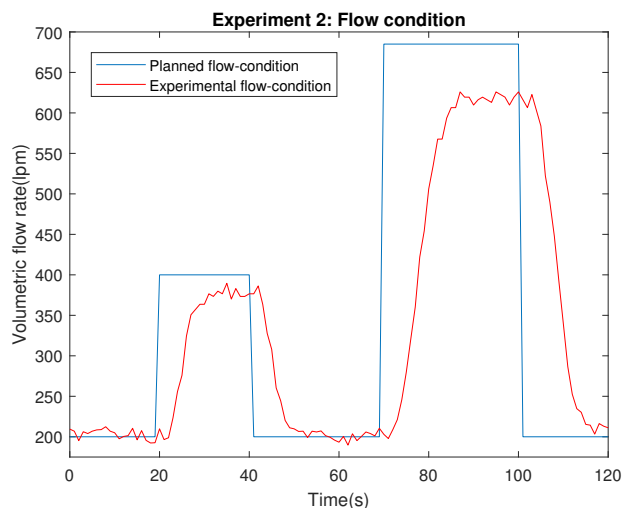


Figure 11.3: Comparison of flow condition

After following the flow condition, result from the thermocouple readings at the different locations of the monolith are presented below. Three trials were done for the proposed flow conditions to reduce experimental errors. The symbol T1 to T8 are the thermocouple numbers. T1 to T4 and T5 to T8 were situated at the outlet and inlet of the monolith respectively, see figure 7.5. It can be seen from the figure 11.4 that the dotted line is slightly higher than fully drawn line, which is showing that the temperatures on the inlet side of the monolith is hotter than the outlet side. This is even more prominent in the blue lined figure with T4 and T8,

where the velocity is expected to be lower and the residence time gave the fluid more time to transport heat through the walls.

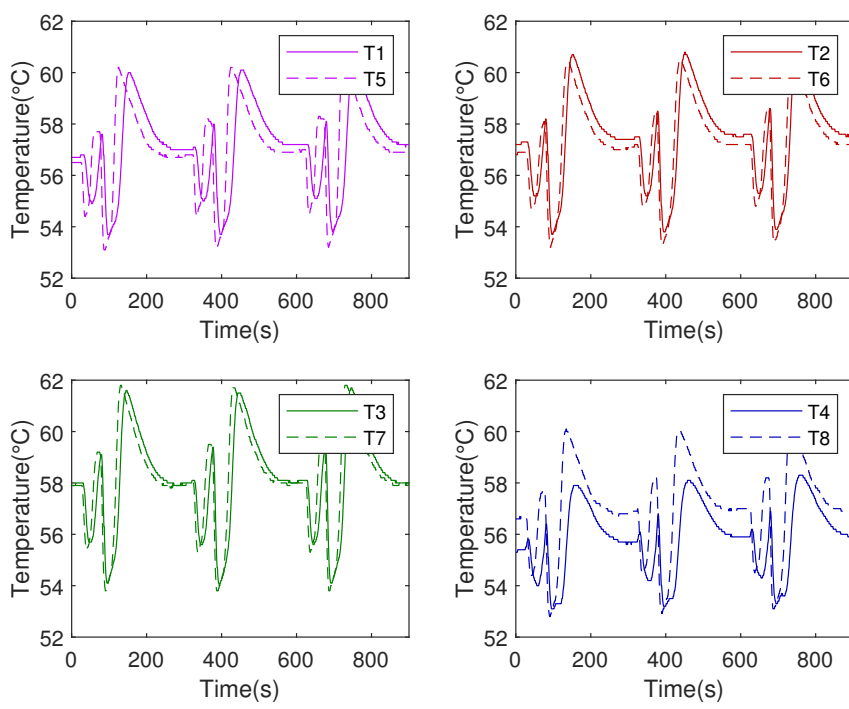


Figure 11.4: Temperature readings at different location of monolith at suggested flow conditions

The graph below shows the temperature readings of T7 sensor at the suggested flow condition and at 60°C reactor inlet temperature for three trials to reduce the experimental error and make sure the results from the experiment are accurate enough. It shows the temperature is low when the flow is high and vice versa, which matches the discussion before in 7.1.

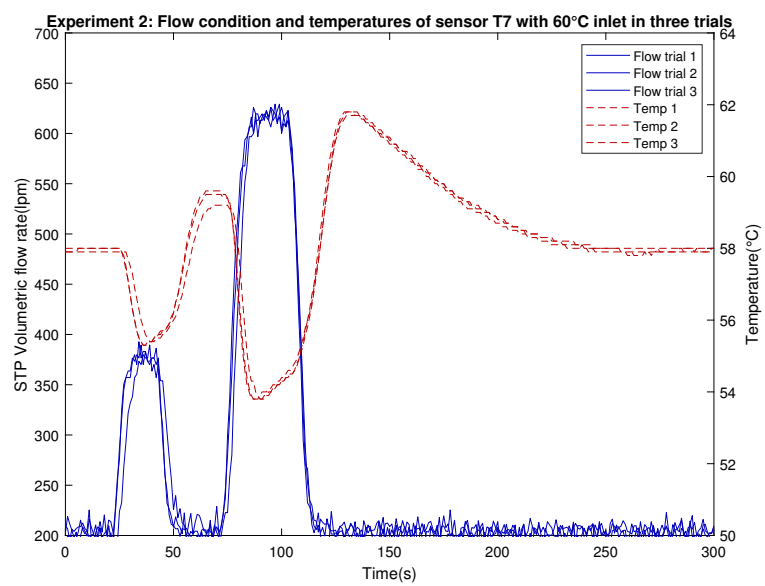


Figure 11.5: Temperature readings of T7 at suggested flow conditions in three trials

11.2.3 Experiment 3a: Reactor Cooling in three flow conditions

The figure below shows the cooling time from 60°C to 25°C at three different flow; low, medium and high. It shows low flow takes longer time to cool down whereas, the high flow takes shorter time because of their respective residence time as expected. Low flow has longer residence time and that is why it needs longer time to cool down and vice versa for high flow.

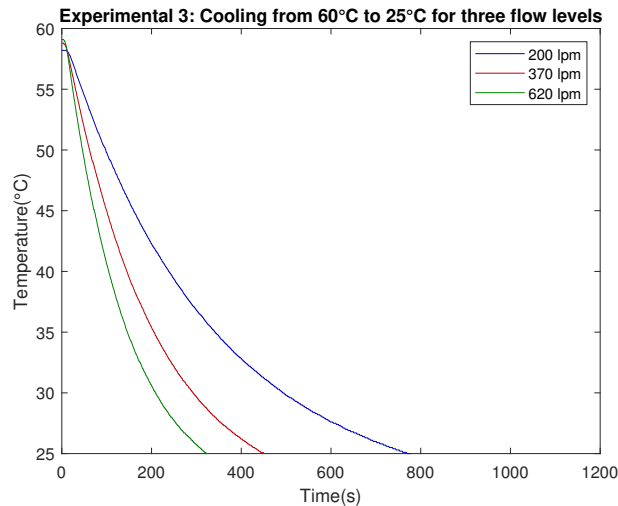


Figure 11.6: Cooling from 60° C to 25° C for three flow condition (low,medium and high)

11.2.4 Experiment 3b: Reactor Cooling in two flow conditions

In this last experiment, the reactor cooling was observed for two flow conditions, high and medium flow sequentially at the highest heating capacity from the heater. This figure has vast amount of information and hard to extract any useful ones only by looking at it. It is presented here just to show the overall trend for the cooling experiment for these two flow conditions. It can be seen from the figure 11.7 that at high flow condition, the temperature reaches approximately 220°C while at medium flow, it reaches till 300°C. The data from this figures will be used to compare the thermocouple readings situated in the inlet and outlet part of monolith between simulation and experiment after the adjustment of simulation model with experimental data. The comparison will be found later on section 11.3.1.

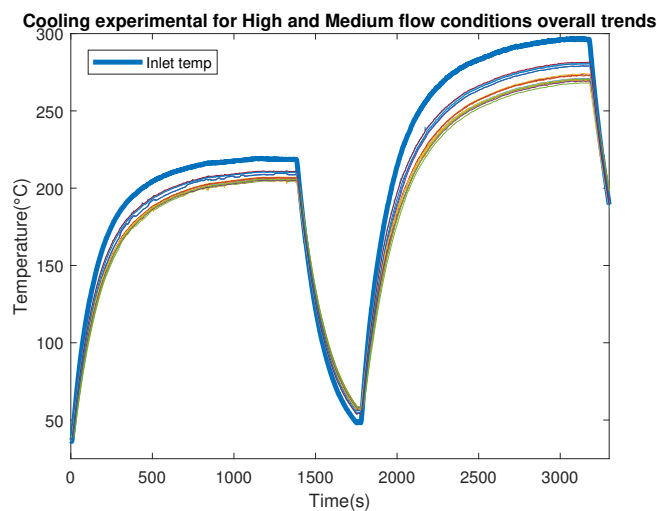


Figure 11.7: Cooling experiment in high and medium flow where the thermocouple readings are shown, specifically for the inlet drawn with a thicker line.

11.3 Adjustments to the model

This section will be divided into smaller parts to describe a step by step procedure in testing and comparing the values between experimental and simulation data. The first step in adjusting the model is done in steady state conditions where the sensors, closest to the inlet are in focus. Aside from reassuring the physical properties of the materials, the main variable to regulate is the heat coefficient term in convection, on the walls between the inlet and monolith.

When the inlet sensors show the same trend of temperature distributions across the inlet, further developments is done by adjusting the thermal conductivity and viscous resistance or inverse absolute permeability of the cordierite monolith as well as convection across the reactor to match the corresponding sensors in the monolith outlet. Finally, the trend for temperature drop between the sensors in the inlet and outlet will be observed to conclude the final validation.

Table 11.3: Summarized settings for the first model in FLUENT.

Models and Conditions	Turbulence model Boundary wall Near-wall model Inlet boundary cond. Outlet boundary cond. Wall boundary cond.	realizable k- ϵ No slip Standard wall function Mass flow-inlet Outflow Free convection at room temperature h=20(inlet), 15(void),5(insulation) [$W/m^2 \cdot K$]
Settings	Mass flow Inlet temperature Inverse absolute permeability Porosity Operating pressure tolerance limit	Transient [kg/s] Transient 2.2 · 10 ⁷ in axial direction 2 · 10 ¹² in radial direction 83% 1 [atm] 1 · 10 ⁻⁶
Air	Density Specific heat Thermal conductivity	Incompressible ideal gas 1.006 [kJ/kg] 0.0242 [$W/m \cdot K$]
Insulation	Density Specific heat Thermal conductivity	380 [kg/m^3] Assumed air Assumed air
Cordierite	Density Specific heat Thermal conductivity	279 [kg/m^3] 1050 [kJ/kg] 1.8 [$W/m \cdot K$] in axial direction 0.9 [$W/m \cdot K$] in radial direction

11.3.1 Comparison of steady state temperatures between experiment and simulation

After adjusting the simulation model to the experimental data, following results are found.

Inlet

In this section, the comparison between experimental and simulation inlet temperature readings are shown. Despite most of the sensors show a similar pattern between experiment and simulation, sensor 8, 11, 10 and 13, shown as violet, green, dotted red and dotted blue respectively, did not follow the experimental pattern. The pattern in the simulation is more logical because it shows 13 has the highest and 8 has the lowest temperature as 13 is in the hottest and 8 is on the coldest zone of monolith. The experiment did not show this probably because of reading error and misplacement of sensors or heat loss in the reactor. Moreover, the thermocouple were inserted from the outlet part of the monolith and travel approximately 7-8 cm inside. As a result, it has been concluded that the wall of the monolith were damaged while the insertion of thermocouples. As a result, the heat conduction of the porous wall were disrupted and showed abnormal results.

Comparison at medium flow condition

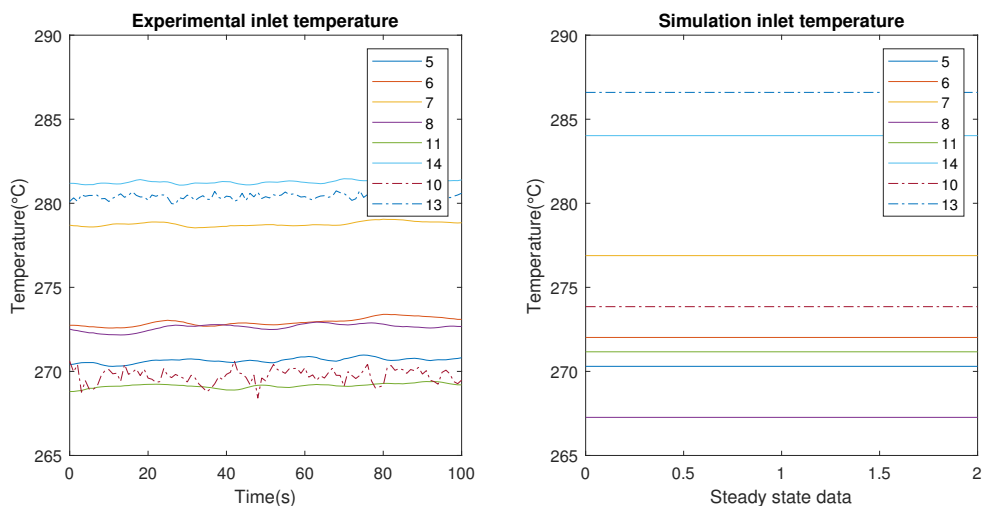


Figure 11.8: Temperature of different sensors in the inlet part of the monolith at medium flow

Comparison at high flow condition

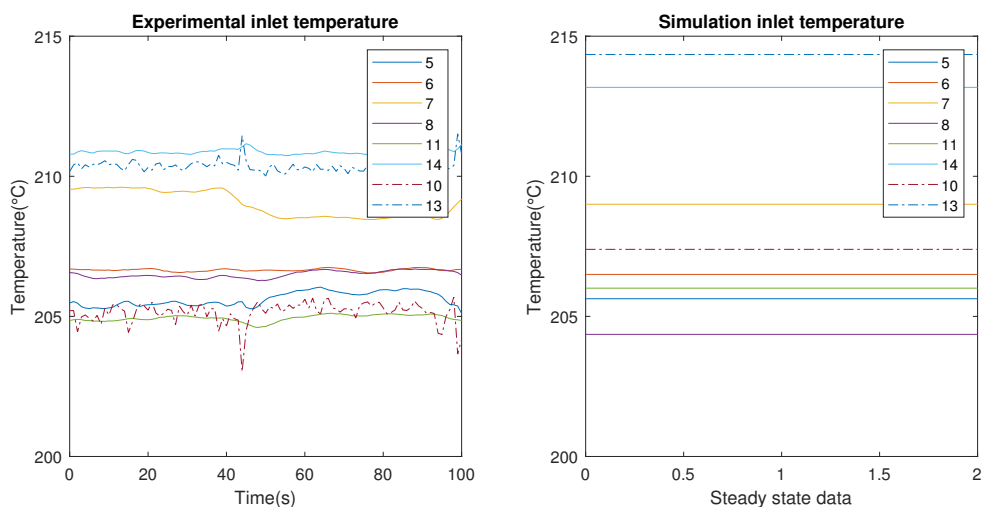


Figure 11.9: Temperature of different sensors in the inlet part of the monolith at high flow

Temperature difference: Inlet-outlet of monolith

The temperature difference between inlet and outlet part of the monolith are described here. Difference between sensors 8-4 and 11-12 do not show similar pattern in experiment and simulation because of the reason discussed in the previous section.

Comparison at medium flow condition

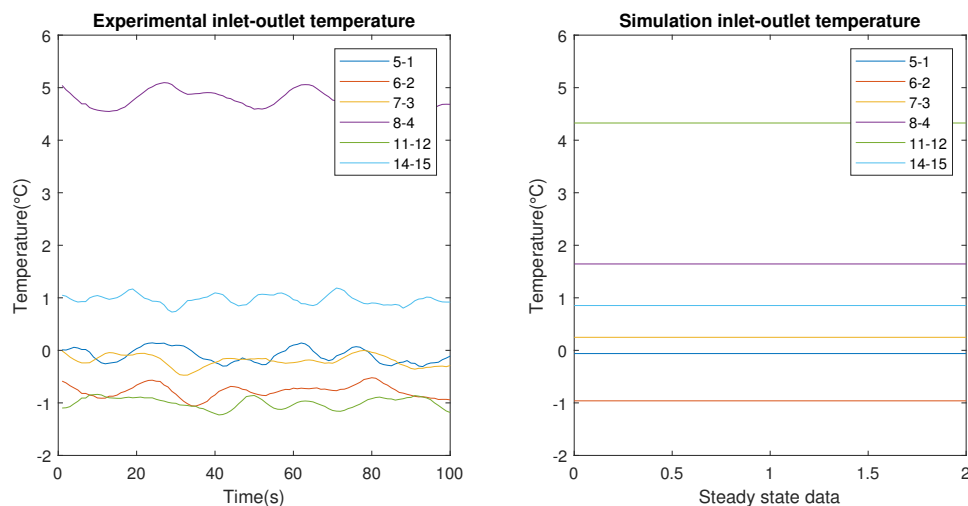


Figure 11.10: Temperature difference in the inlet and outlet part of the monolith at medium flow

Comparison at high flow condition

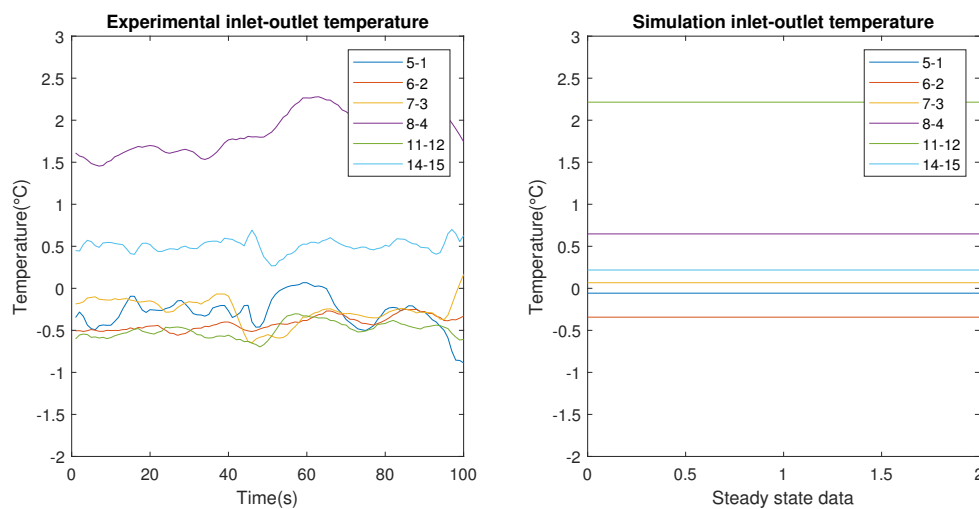


Figure 11.11: Temperature difference in the inlet and outlet part of the monolith at high flow

Outlet

Finally, in this section, it can be seen that the temperature readings of the sensors at the outlet face of monolith show an exact similar pattern in the simulation as in the experiment. The pattern matches pretty well enough because of the placement of the sensors properly. All the sensors were inserted 1-2 cm inside from the outlet part of monolith; and the thermocouple wires did not travel longer path and as a result, the monolith wall stayed intact. There is a deviation of 2 to 3°C in each sensors between experiment and simulation model, which is a minor error to the adjusted model.

Comparison at medium flow condition

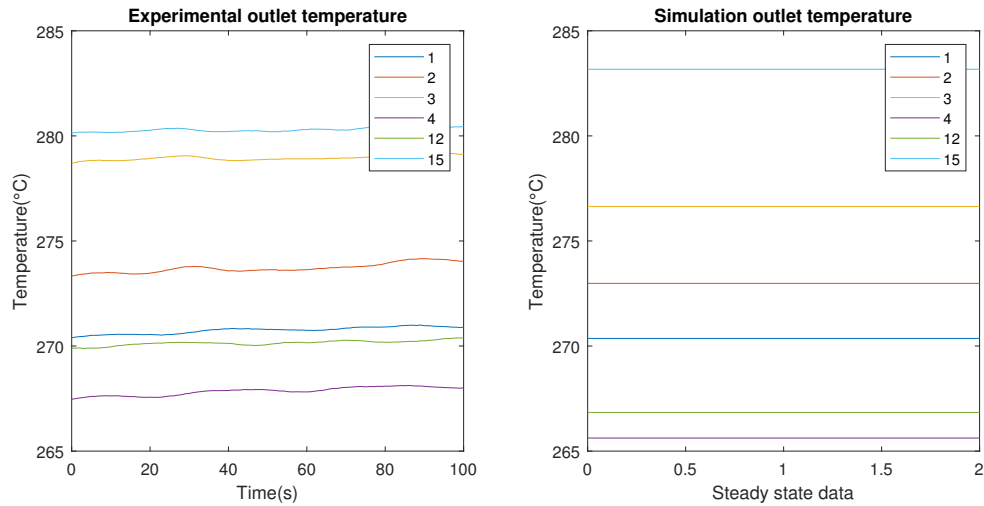


Figure 11.12: Temperature of different sensors in the outlet part of the monolith

Comparison at high flow condition

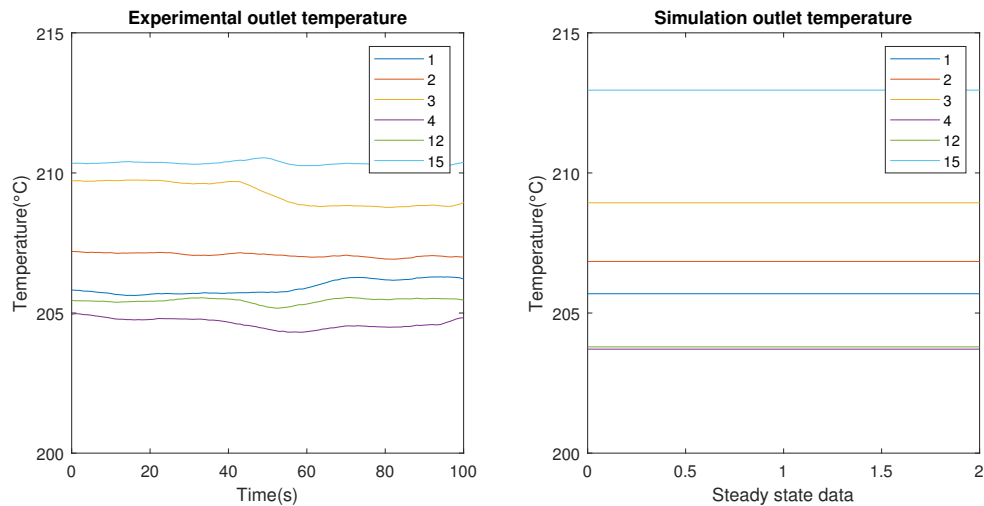


Figure 11.13: Temperature of different sensors in the outlet part of the monolith at high flow

11.3.2 Transient cooling

The cooling procedure in experiment 3b takes too long time to reach room temperature, even for high flows. Instead, the simulation will only be done on the first 20-30 seconds of the cooling experiment where the temperature change is the highest. Two simulations will be done for medium and high flows respectively, to conclude the final parameters in the model.

11.4 Optimal sensor locations

An optimal set of sensors has been chosen among 82 predefined locations in the outlet of the monolith, by using D-optimal design on a PCA model. The set of locations varies depending on which simulation case is used in creating the PCA model. The results of these will be shown in the following subsections.

11.4.1 Potential sensor placements

The points for which the potential sensor location were spread across the face of monolith outlet are shown below in figure 11.14. 82 different possible locations were defined in the half plane while assuming symmetry for the other half, avoiding multiple sensors at identical position on the other side.

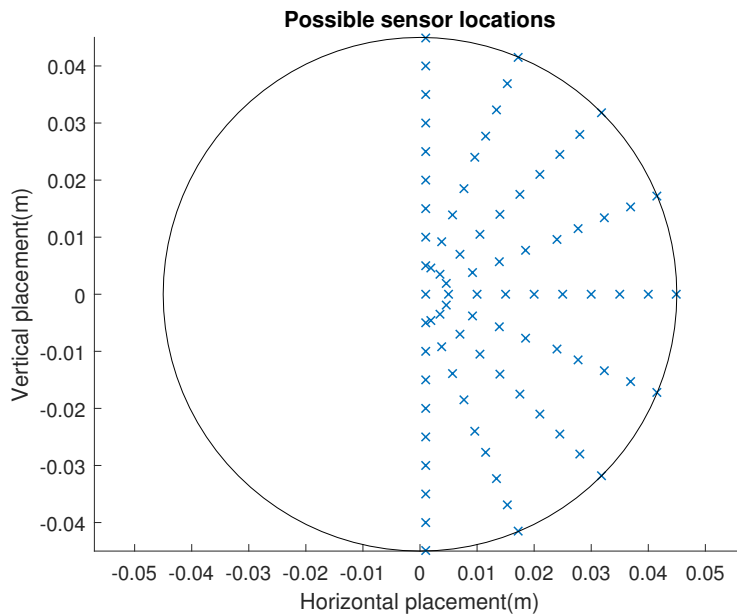


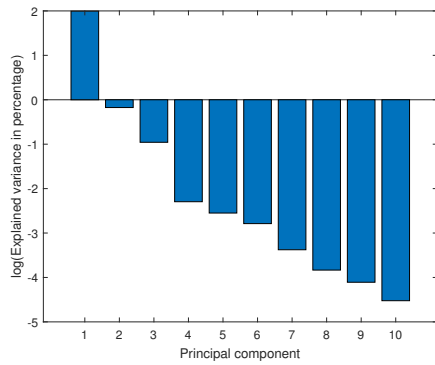
Figure 11.14: A display from the monolith outlet with the 82 possible sensor locations.

As earlier mentioned, an assumption for the area which every sensor covers was divided evenly across the outlet for the calculation of the weighting factors. It is clearly not the best assumption for the placements of the depicted potential locations, but since the idea to implement both velocity and temperature into one model was introduced after the placements and generation of simulation data. It would require time to re-locate and simulate new data with i.e. equidistant points etc.

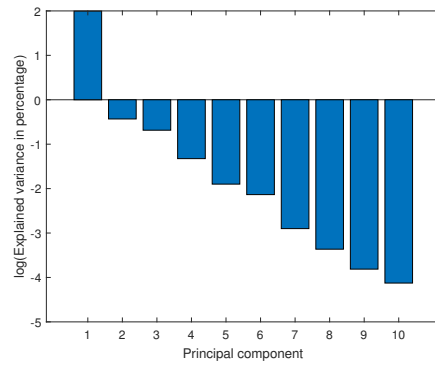
11.4.2 Principal component analysis

The principal component analysis is conducted on the three simulation cases discussed in earlier sections. Unit variance scaling is used on the data, so that the the sum of the explained variance over the maximum number of principal component results in 100%. By choosing a lesser number of PCA's, the model matrix loses accuracy by gaining calculation speed. Thus, it is of interest to find a balance between accuracy and speed by experimenting with the number of components.

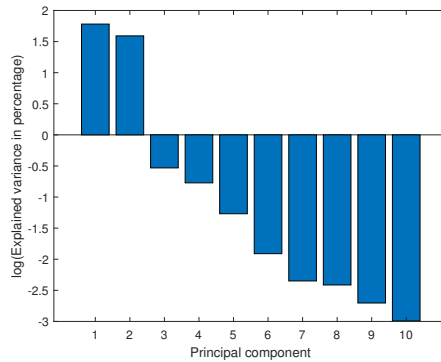
Comparing the models, consisting of a single variable and the heat flux model, it becomes apparent that the two-variable model require more PC's to explain the variance. Since both temperature and velocity data is taken into account, it needs two PC's to cover for the majority of the variances while the respective single variable ones only need one component.



(a) *PC's for velocity.*



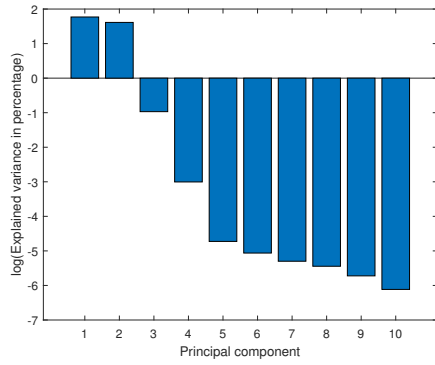
(b) *PC's for temperature.*



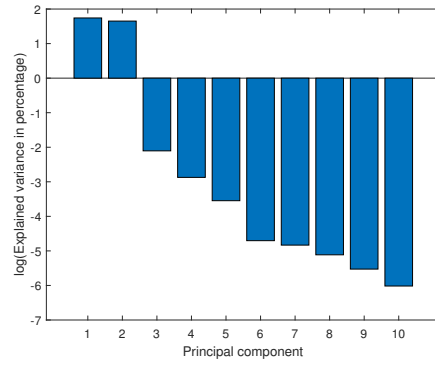
(c) *PC's for heat flux model*

Figure 11.15: *Principal components ordered after most variance explained, from driving cycle case.*

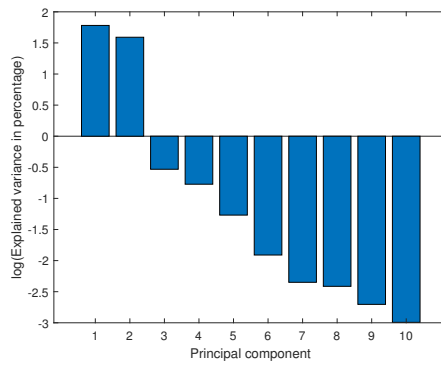
As shown on figure 11.16 below, the most impactful principal components are the first two which have a magnitude above 1 for all simulation cases, when both temperature and velocity variables are considered. After the first two, the majority of the explained variances rapidly decrease. Depending on the targeted accuracy of the model, it can be enough to use two components which can explain the majority of the variances. However, a sufficient number of PC's are needed for the algorithm to determine 4 different locations. Further more, it is shown in the bar graphs that the importance of adding additional PCs beyond two varies, depends on which case is observed.



(a) *Cooling in high flow, variances explained $\geq 99.9\%$ with 2 PCs*



(b) *Cooling in medium flow, variances explained $\geq 99.9\%$ with 2 PCs*



(c) *Driving cycle simulation at 60°C, variances explained $\geq 99.9\%$ with 4 PCs*

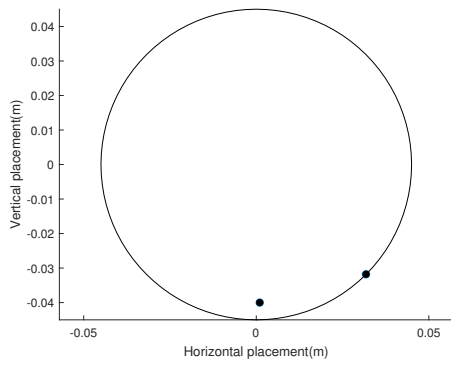
Figure 11.16: A logarithmic scale of the explained variance for the ten first principal components, for the three different flow cases.

11.4.3 D-optimal design

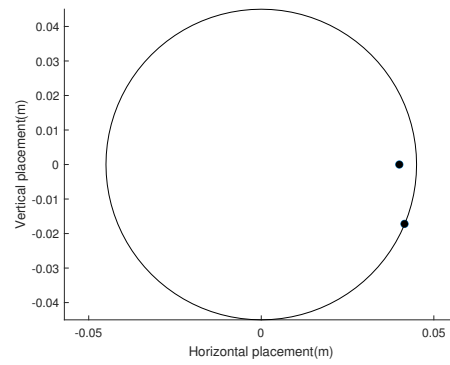
Three cases of optimal sensor locations, high and medium cooling and driving cycle experiment respectively, are tested. The project goal was to use a maximum of 4 sensors to capture the state of the reactor. Thus, a lesser number of sensor would also have to be tested and compared with the maximum. Further more, it is also of interest to see how many principal components should be used to to achieve a better accuracy without losing too much on calculation time and vice versa.

A test was conducted on 3, 4 and 5 component PCA to find the best four sensor locations for the driving cycle case, where the RMSE was observed, $RMSE = 0.0441, 0.171$ and 0.0230 respectively. For the three tests, 100 iterations and 100 tries was needed to assure a D-optimal is found every time the code is rerun. An additional test on 10 PCs was conducted which in it's best resulted in $RMSE = 0.0139$. However, the result was not identical for every run, even when using 1000 iterations and 1000 tries, which concluded that using too many PC's would cause an uncertainty in the results. Since the best and most reliable result was achieved with 5 PC's, the proceeding simulations and tests are done with 5 principal components.

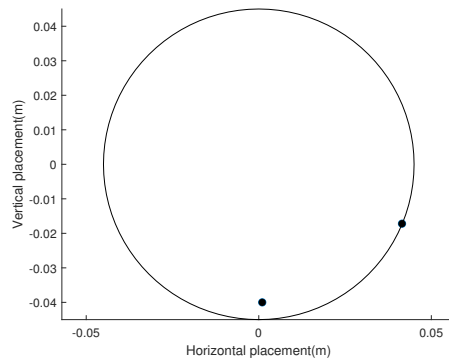
A comparison study between the two-variable model for temperature and velocity and one-variable, for temperature and velocity respectively, is conducted. The goal is to see how the model accommodates for the two parameters, since respective optimums are most likely not in the same place. To make it more visible to see how the heat flux model chooses the locations based on both temperature and velocity, a lesser number of sensors is initially used. In figure 11.17, it is apparent that the two locations the heat flux model has chosen are divided such that each sensor belongs to one optimal of each variable.



(a) Two best locations for a 5PC model on velocity data.



(b) Two best locations for a 5PC model on temperature data.

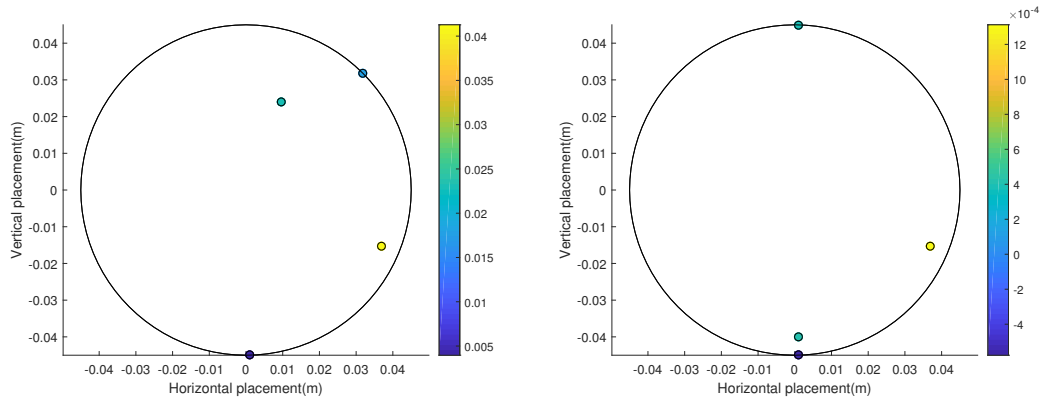


(c) Two best locations for 5PC model on heat flux.

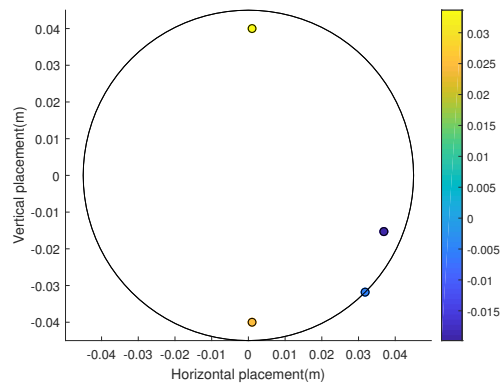
Figure 11.17: For a model with only two sensors, the heat flux model chooses two locations which is identical to one optimal location for each variable.

Earlier in the principal component analysis, it was shown that the driving cycle case, benefits the most from using more PC's according to figure 11.16. Thus, the attempts to find a good accuracy for all models was done with regard to the worst case, the driving cycle.

The results below show the four optimal locations for each separate case, coloured after the weight factors. As expected, the four optimal locations in each case are not identical, since the temperature changes are much more significant in high and medium flow compared to the driving cycle simulation. However, there are similarities in the optimal location which possibly means an overall optimal location exist close to these points. For instance, there exist an optimal sensor close to the bottom part of the monolith, which is where the velocity is expected to be the highest, see figure 11.1b. Same goes for the location at four o'clock position which is also an optimal for all cases which can be the result of being in the a high fluctuating region for both temperature and velocity during the transient states.



(a) High flow, UV-scaling, $RMSE=2.10E-2$ (b) Medium flow, UV-scaling, $RMSE=4.5E-2$



(c) Driving cycle simulation at $60^\circ C$, UV-scaling, $RMSE=2.30E-2$

Figure 11.18: The optimal four locations for the 3 different cases with respect to both velocity and temperature. The colorbar shows the weight factor for the corresponding location.

The RMSE was also showing a declining trend as more sensors were put into the model since higher order of freedom is granted. Thus, to finalize the D-optimal design for locating the sensors, it was concluded that 5 component PCA was sufficient to explain most of the variances when using four sensors.

The model parameters that were found, were different for each flow condition. Thus, it was of interest to test each model on the other cases and will be depicted below.

It is apparent that the accuracy of the model is strictly based on the actual case. However, as the high flow

Table 11.4: A compilation of performance for each model, depending on various flow conditions. The shown values is the RMSE of actual and modelled outlet heat flux.

Calibration\Case	High flow	Medium flow	Drive cycle
High flow	0.021	3.76	153.0
Medium flow	7.170	0.045	151.3
Drive Cycle	108.7	61.84	0.023

and medium flow cooling experiments are of similar fashion, the RMSE is much smaller between the two. The RMSE when using the model parameters for the drive cycle case, shows large errors when used on the cooling cases and vice versa. The logical explanation to this, is that the driving cycle has more variation in velocity while the cooling cases varies in temperature.

12 Conclusion

This Master's thesis dealt with the CFD modelling study of exhaust gas flow behavior from combustion engine in a monolithic reactor of EATS system. The velocity and temperature profiles inside the monolith were observed in the laboratory experiment, which was then used to adjust the CFD model. The adjusted ideal model was then used to get the optimal locations of the sensors. The purpose of installing the sensors in optimal locations was to define the state of the system of the reactor.

To adjust the CFD model with laboratory experimental data, tuning various parameters were conducted. These include using different wall heat conduction coefficient for different part of domain, heat convection inside the monolith and viscous resistance (inverse absolute permeability) of the cordierite monolith. It was observed that the velocity and the temperature were highest at the middle bottom part of the monolith as most of the flow go through that part. These profiles were lower gradually in the middle upper part and close to the wall of monolith.

The design to find the optimal locations to place temperature and velocity sensors have been found, with fixed number of potential sites. Since the design was done via simulations, it is possible to redesign the potential placements such that it can have more freedom and also to reduce the error in the area assumption. Nevertheless, whether a sensor can capture both velocity and temperature or only one of the parameters, the optimal location can be found by using the developed code. The final optimal set was chosen as set of four locations with consideration to temperature and velocity data. Four PC's were used when conducting the model, as this guarantees 99.9% captured variance for the three cases. Thus, depending on which flow condition was used, the RMSE for the model varied between $2E - 2$ to $7E - 2$.

Though they were many considerations which could not be taken into account for simplicity and insufficient time, scope of future work to continue from here and few recommendations for improving the this study are discussed in the later sections. Otherwise, it can be said that the purpose of this Master's thesis project to develop an accurate CFD model to represent an actual reactor to simulate and find the optimal locations has been achieved.

13 Recommendations

While doing this master's thesis, some complications were faced. But these complications can be override by the recommendations discussed below. First of all, CFD modelling is a very tricky part of CFD studies. Understating the physics behind every small detail was crucial otherwise the simulation result would end up as a trash. Getting reliable data for various parameters such as monolith characteristics data, the heat conduction data for the reactor wall and the insulation material were very essential to get accurate results. As a result, getting the data from authentic sources and verify them is the first recommendation provided.

Secondly, while performing the laboratory experiment, installing the thermocouples were a burdensome job to do. Finding good locations in the monolith where they can observe the most gradients as well as putting them inside the monolith without breaking the wall were the reason for this struggle. Besides, the monolith was installed from the outlet part, so they travel 7-8 cm inside the monolith to get the data from inlet and 1-2 cm to get data from outlet approximately. These installation of thermocouples were done completely on guessing how much deep they are inside, which is not proper scientific way. Thus the first recommendation here would be the proper approximation of thermocouple locations in the monolith so that they can get the necessary information without having any unnecessary waves of data. The second recommendation could be the installation. Inserting the thermocouples was tricky as they were travelling inside the channels and the walls are pretty much fragile. In the experiment, it was done very carefully still some surface of the walls were fractured. The walls break easily by the friction of thermocouples. So inserting them slowly and properly without destroying the wall while setting up the experiment would be an important recommendation.

Finally, the last recommendation would be the adjustment accuracy of CFD model with the laboratory experiment. The sensor locations in the CFD model was also an approximation and didn't quite match with the laboratory experimental locations of the thermocouples. This matching is very much important to mimic the temperature profiles in the CFD model accordingly. As a result, getting a fixed location for thermocouples and install them as similar as possible would be the third recommendation. These recommendations will assist to achieve a better CFD modelling of EATS system by having a model representing reality more accurately. A few examples of such changes are as follows:

- Area coverage per sensor dependent on the distance from center
- Re-evaluate and compare scaled versus unscaled parameter matrix.
- Consider other models than the current first order model by adding correlated terms and higher order terms in the parameter matrix.

14 Future work

This Master's thesis was completed within 24 weeks. So to say, lack of time was an huge factor not to design a model with all the considerations of exhaust treatment system. As a result, a lot of considerations were not covered fully in this project. This project is the starting of a bigger research interest. Since it will continue in the future, findings from this will be a crucial initial base for that.

Like mentioned before, the goal of the project was mainly understanding the behavior of the flow such as the velocity and temperature distribution inside a monolith of a reactor, reactions of the exhaust gases were not taken into consideration here. It was questionable to assume pure air as exhaust gases having no exhaust gas substances in it, which is absolutely not true in real case scenario. Still this consideration was taken for the sake of simplicity. So, it can be said that taking catalytic reactions in account will be a pretty interesting step as a future work to this project.

The provided monolith was a catalyst substrates made from cordierite which is very popular to use in emission control technology. Besides, a comparison study for other catalyst material which can be more efficient than cordierite in emission control purposes can be a good future work. A study of different monolith substrates can be done in the future to observe which substrate is better for different kind of exhaust gas removal.

The heater used in the laboratory for heating the inflow air had a maximum capacity of only 3kW. This is moderately low as it can only heat the air up to 860°C, at very low flows. A study of using more powerful heater to reach a very high exhaust temperature and observe the temperature profiles in the monolith would be a fascinating experiment to do. This can reveal how different monolith react at a very high temperature scale and will help achieve a better understanding on experimental heating limitations.

The pressurized air in the laboratory had a limit of 60 000 space velocity, when flowing across the equipment. As earlier mentioned, this is about as low as a vehicle will go, while it also is the highest reachable flow in this case. It would be interesting to know how the model fares in space velocities closer to the upper bound of real vehicles, and what modifications would have to be made to further advance the model.

Moreover, the D-optimal study done in this project was not quite satisfactory as three different sets of optimal sensor locations were found for three different experimental procedure. A single set of optimal sensor locations for all the experiments would be the best scenario. It is possible that the optimal placement, which depends on the data that was gathered, are different depending on how the data look, so the optimal locations varied with experiments.

Finally, it would be very interesting to simulate a much longer driving scenario with much wider temperature and flow range to finally see if there is an improved model performance for the other cases.

References

- [1] Intergovernmental Panel on Climate Change. *Climate Change 2014 Synthesis Report - IPCC*. 2014. ISBN: 9789291691432. DOI: 10.1017/CB09781107415324.
- [2] İbrahim Aslan Reçsito\uglu, Kemal Altini\csik, and Ali Keskin. The pollutant emissions from diesel-engine vehicles and exhaust aftertreatment systems. *Clean Technologies and Environmental Policy* **17.1** (January 2015), 15–27. ISSN: 1618-9558. DOI: 10.1007/s10098-014-0793-9. URL: <https://doi.org/10.1007/s10098-014-0793-9>.
- [3] World Health Organization (WHO). *World Health Statistics 2018: Monitoring Health for the SDGs, Sustainable Development Goals*. Tech. rep. 2018.
- [4] Jana Aslanjan et al. “Simulation of a Three-Way Catalyst Using Transient Single and Multi-Channel Models”. *SAE Technical Paper Series*. 2017. DOI: 10.4271/2017-01-0966.
- [5] DieselNet. Cellular Monolith Substrates. *DieselNet Technology Guide* (1998). URL: https://www.dieselnets.com/tech/cat_substrate.php (Accessed on: January 30, 2019).
- [6] Bengt Andersson et al. *Computational fluid dynamics for engineers*. 2011. ISBN: 9781139093590. DOI: 10.1017/CB09781139093590.
- [7] Richard Stone. *Introduction to Internal Combustion Engines*. London: Macmillan Education UK, 1992, pp. 1–271. ISBN: 978-0-333-55084-7. DOI: 10.1007/978-1-349-22147-9.
- [8] Arcoumanis. Dicos. “INTERNAL COMBUSTION ENGINES”. *A-to-Z Guide to Thermodynamics, Heat and Mass Transfer, and Fluids Engineering*. Begellhouse. DOI: 10.1615/AtoZ.i.internal{_}combustion{_}engines. URL: <http://www.thermopedia.com/content/880/>.
- [9] Adam Forrest. *The death of diesel: has the one-time wonder fuel become the new asbestos? — Cities — The Guardian*. 2017. URL: <https://www.theguardian.com/cities/2017/apr/13/death-of-diesel-wonder-fuel-new-asbestos> (Accessed on: January 25, 2019).
- [10] John B Heywood. *Internal Combustion Engine Fundamentals*. 1988, pp. 42–659. ISBN: 007028637X.
- [11] Ulrich G. Alkemade and Bernd Schumann. Engines and exhaust after treatment systems for future automotive applications. *Solid State Ionics* **177.26-32** (October 2006), 2291–2296. ISSN: 0167-2738. DOI: 10.1016/J.SSI.2006.05.051.
- [12] Kim Nguyen. *Volvo Exhaust After treatment - YouTube*. 2016. URL: <https://www.youtube.com/watch?v=a6k55eeuw0U> (Accessed on: September 4, 2019).
- [13] Hannes Kannisto. *Exhaust aftertreatment system - a cleaning process for exhaust*. 2017. URL: <http://nordicblog.volvopenta.com/exhaust-aftertreatment-system-cleaning-process-exhausts/> (Accessed on: January 30, 2019).
- [14] Eckard Helmers and Patrick Marx. Electric cars: technical characteristics and environmental impacts. *Environmental Sciences Europe* **24.1** (April 2012), 14. ISSN: 2190-4715. DOI: 10.1186/2190-4715-24-14. URL: <https://doi.org/10.1186/2190-4715-24-14>.
- [15] T. J. Barlow I. S. McCrae and S Latham P. G. Boulter. A reference book of driving cycles for use in the measurement of road vehicle emissions. **PPR 354** (2009). URL: https://www.gov.uk/government/uploads/system/uploads/attachment_data/file/4247/ppr-354.pdf.
- [16] Emilia Silvas et al. Synthesis of Realistic Driving Cycles With High Accuracy and Computational Speed, Including Slope Information. **65.6** (2016), 4118–4128. ISSN: 18671306. DOI: 10.1007/s12602-012-9117-8.
- [17] Michiel Makkee Suresh T. Gulati and Agus Setiabudi. *Structured Catalysts and Reactors*. Ed. by Andrzej Cybulski and Jacob A. Moulijn. 2nd. Boca Raton, FL, USA: CRC Press, Taylor & Francis Group, 2006. ISBN: 9780824723439.
- [18] *ANSYS Fluent Theory Guide*. Tech. rep. 2013. URL: <http://www.pmt.usp.br/ACADEMIC/martoran/NotasModelosGrad/ANSYS%20Fluent%20Theory%20Guide%2015.pdf>.
- [19] *ANSYS Fluent User’s Guide*. Tech. rep. 2013. URL: <http://www.pmt.usp.br/academic/martoran/notasmodelosgrad/ANSYS%20Fluent%20Users%20Guide.pdf>.
- [20] J.O. HINZE. *Turbulence: McGraw-Hill Series in Mechanical Engineering*. 2nd. New York: McGraw-Hill College, 1975, p. 790. ISBN: 978-0070290372.
- [21] B. E. Launder and D. B. Spalding. *Lectures in Mathematical Models of Turbulence*. 1972. ISBN: 0124380506.
- [22] R. E. Hayes et al. “CFD modelling of the automotive catalytic converter”. *Catalysis Today*. 2012. DOI: 10.1016/j.cattod.2012.03.015.

- [23] Fredrik Ekström and Bengt Andersson. “Pressure Drop of Monolithic Catalytic Converters Experiments and Modeling”. 724. 2002. ISBN: 9780991556700. DOI: 10.4271/2002-01-1010. URL: <http://papers.sae.org/2002-01-1010/>.
- [24] George W Roberts. *Chemical Reactions and Chemical Reactors*. First. Raleigh: John Wiley & Sons, 2008, pp. 47–48. ISBN: 978-0471-742203.
- [25] Zakaria Jaadi. *A step by step explanation of Principal Component Analysis*. URL: https://towardsdatascience.com/a-step-by-step-explanation-of-principal-component-analysis-b836fb9c97e2?fbclid=IwAR3weSn8YBf_K5aUXxenGiwx5Tr5NK4uFlwztzJKzaTD95hcvwzsU0vWb8 (Accessed on: May 16, 2019).
- [26] *D-Optimal Designs - MATLAB and Simulink - MathWorks Nordic*. URL: <https://se.mathworks.com/help/stats/d-optimal-designs.html> (Accessed on: May 16, 2019).

A Appendix A

A.1 Expected highest temperature in the monolith outlet

Expected temperature in the outlet of the monolith (maximum 560K or 287°C) from the simulation with a STP volumetric flow rate of 513 lpm and 571K (298°C) temperature in the reactor inlet.

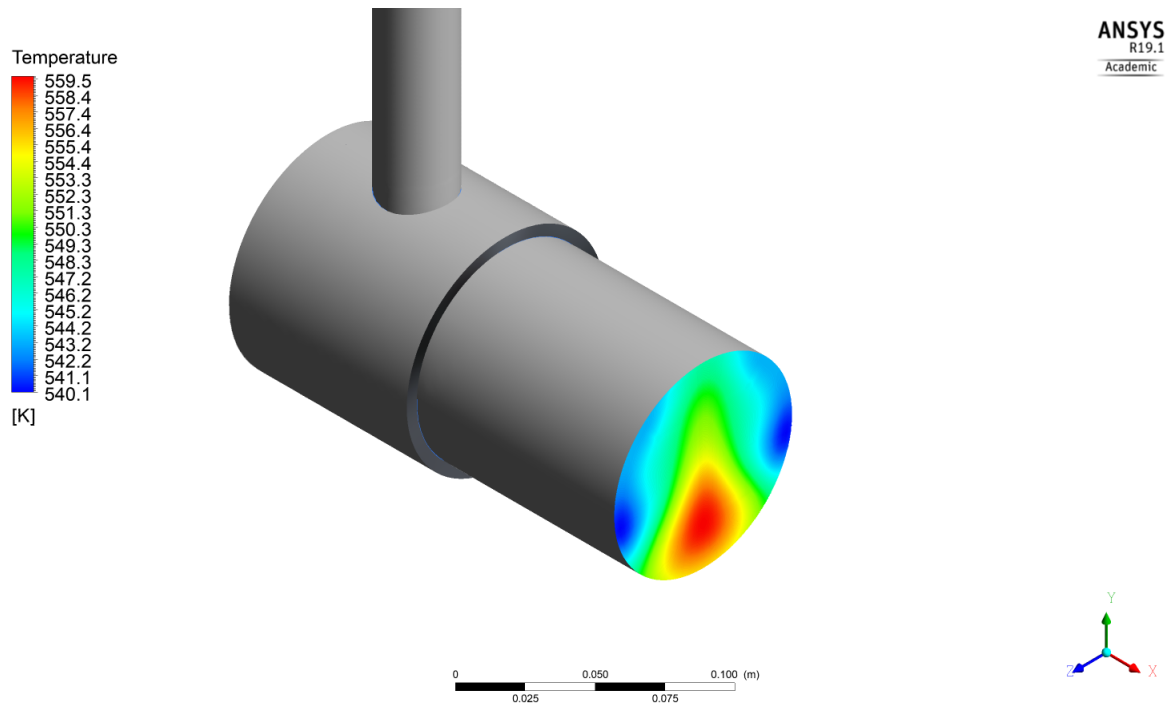


Figure A.1: Catalytic converter with simulated outlet temperature profile.

A.2 Experimental Risk analysis

Activities/Experimental Components	Risk source/possible consequences	Risk Classification			Measures for risk prevention/minimization
		Impact (X) × Probability (Y) = Risk (Z) Scale: 1 to 4			
		X	Y	Z	
1. Pressurized workshop air	Disconnecting pipes when there is high pressure inside can create strong impulse and scatter objects in the lab.	3	1	3	Level out the pressure and close the valve before attaching/disconnecting pipes.
2. Pressure Regulator	Pressure fluctuations can cause harm to the equipment. It is connected with an orifice which causes noise, being in excessive noise for a long time can cause damage to the ear drum	3	2	6	Regulate the pressure cautiously and steadily. Wear noise-protection
3. Laminar air flow element	No risk	1	1	1	No prevention
4. Heater	Breakage or misconnection of the electrical wires can cause electric shock and the wires can be flammable. Tripping on the electrical wires on the floor.	4	3	12	Put the wires behind the equipment and avoid using sharp objects while connecting the wires to power source. Avoid having too many wires lying on the floor without proper taping or attach them on the ceiling. Do not forget to turn off heater when the experiment is over.
5. Bend pipe	Hot air flows through and is cooled only by free convection. Can be very hot to touch.	2	2	4	Wear gloves or avoid putting your hands on the pipe.

6. Catalytic reactor with thermocouples	Hot air flows through and is cooled slightly by free convection and the heat leaves the reactor into the surroundings. The reactor can be very hot to touch.	2	2	4	Wear gloves while putting hands on the reactor. If the surrounding temperature becomes too high, stop the experiment and wait for cooldown.
7. Prandtl tube	It is close to the outlet where there can be direct contact to the heated air. For low air flows and high heating load, the temperature can be sufficient to cause burning.	3	2	6	Adjusting the placement for prandtl tube can be done with heat protection. While it is measuring, one can take a step away from the outlet. For low flows, the temperature can be very high. Can measure the low flows without heating.
8. Air Outflow	The air coming from the outflow goes to the surroundings can cause burning as it will be very hot.	3	2	6	Wear heat protection and always approach the outflow slowly.

B Appendix B

B.1 Mesh

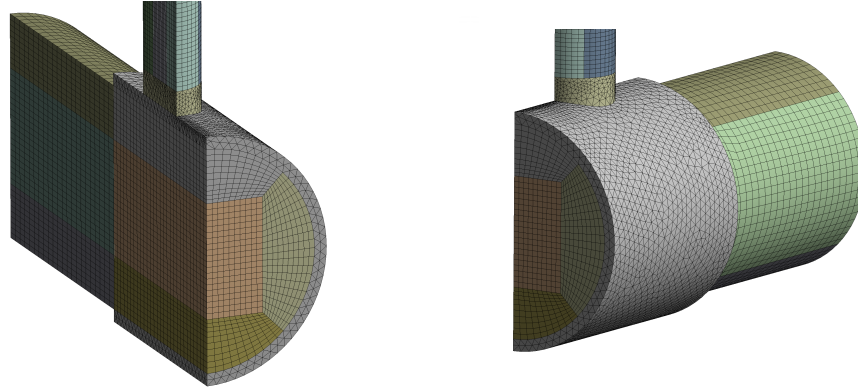


Figure B.1: *Side view of the meshing of the domain*

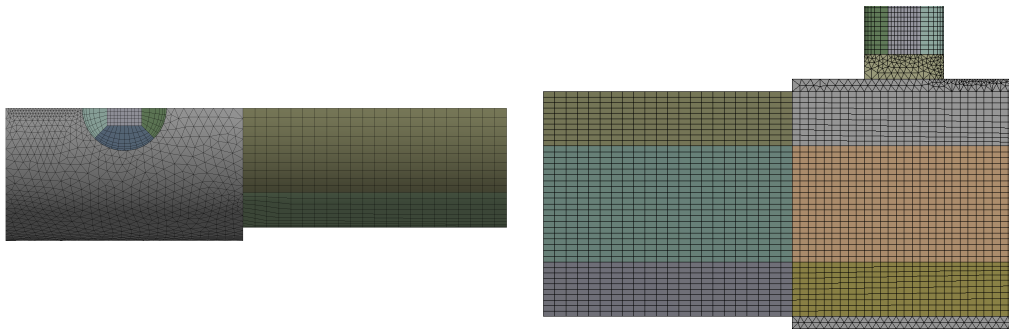


Figure B.2: *Meshing of the topview and inside part of domain*

B.2 Grid independence study: Velocity distribution

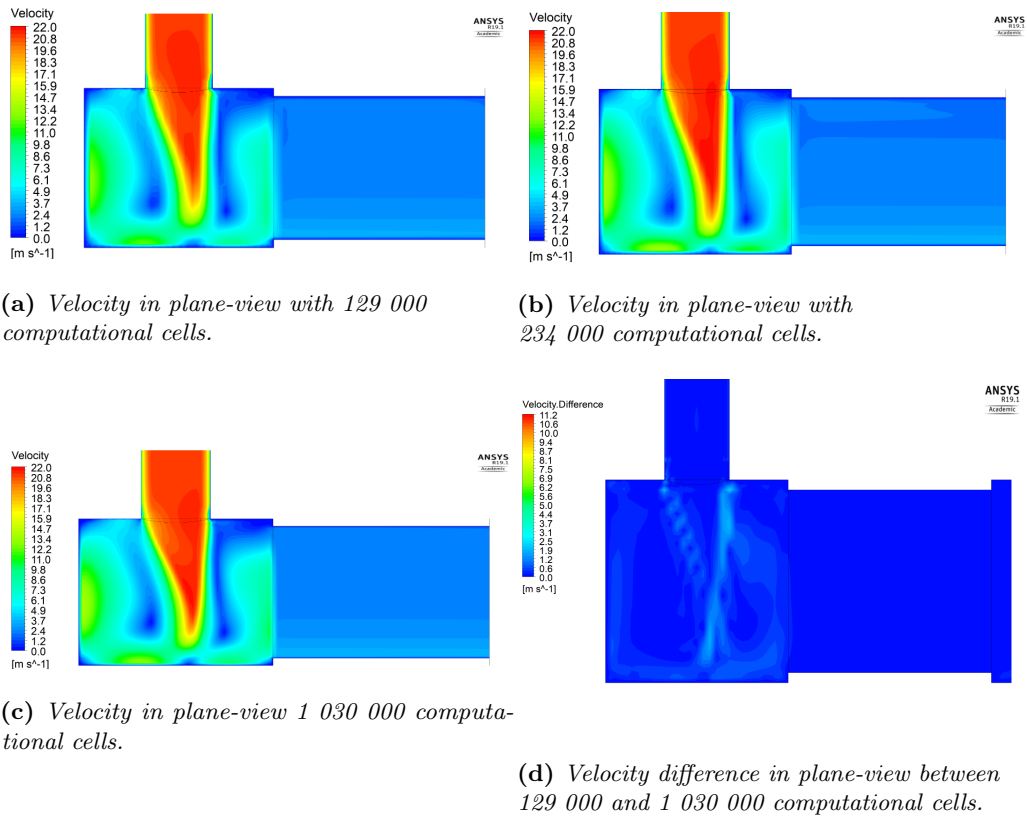
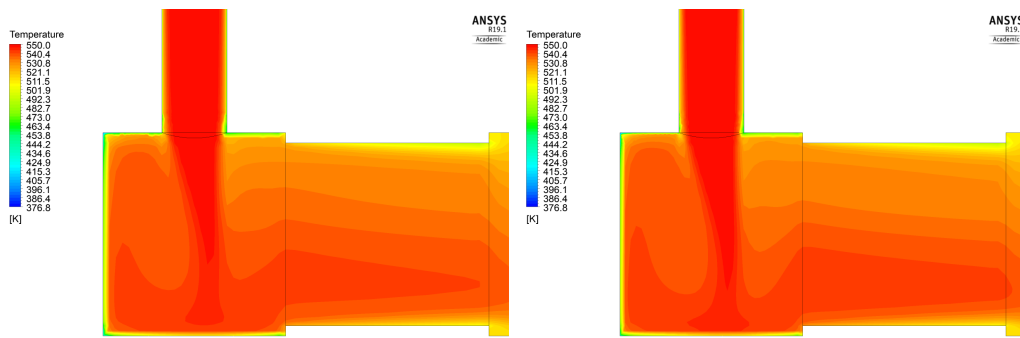


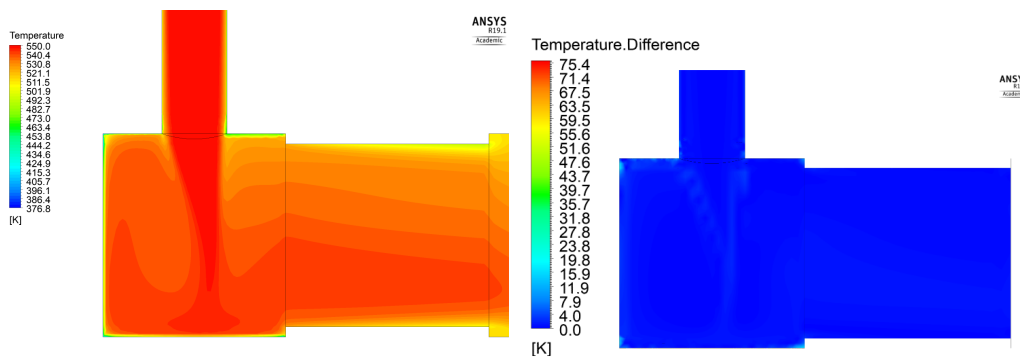
Figure B.3: The grid independence study which 3 respective cases show no significant difference in velocity distributions.

B.3 Grid independence study: Temperature distribution



(a) Temperature in plane-view with 129 000 computational cells.

(b) Temperature in plane-view with 234 000 computational cells.



(c) Temperature in plane-view with 1 030 000 computational cells.

(d) Temperature difference in plane-view between 129 000 and 1 030 000 computational cells.

Figure B.4: The grid independence study which 3 respective cases show no significant difference in temperature distributions.

C Appendix C

C.1 Additional Figures

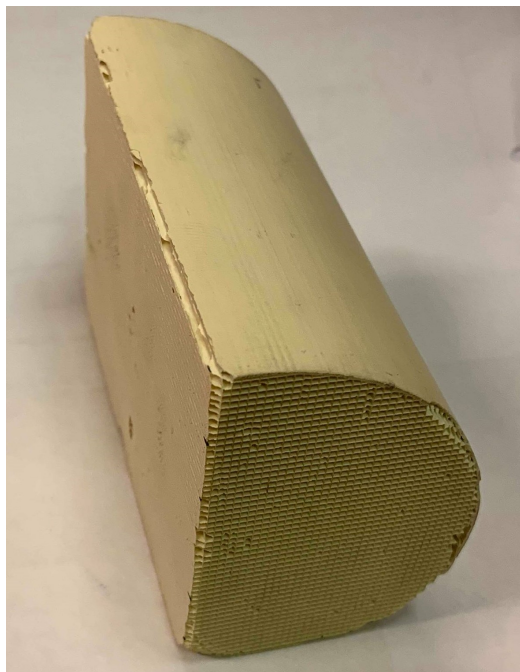


Figure C.1: *Cordierite Catalyst, used in the reactor*



Figure C.2: *Photo of the reactor*



Figure C.3: *The reactor, mounted in the laboratory*

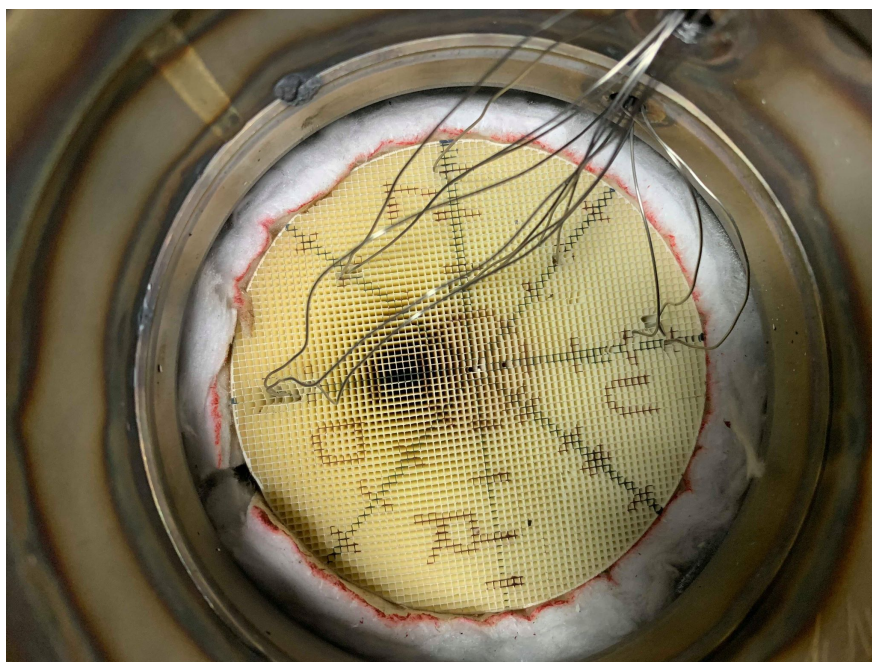


Figure C.4: *Photo taken from the reactor outlet, containing Cordierite catalyst, which is supported by glass wool insulation material, with thermocouple inserted in it*